remote sensing

MDPI

Article

An Integrated Remote-Sensing and GIS Approach for Mapping Past Tin Mining Landscapes in Northwest Iberia

João Fonte [1,*], Emmanuelle Meunier [2,3], José Alberto Gonçalves [4], Filipa Dias [4], Alexandre Lima [4], Luís Gonçalves-Seco [5] and Elin Figueiredo [2]

1 Department of Archaeology, University of Exeter, North Park Road, Exeter EX4 4QE, UK
2 CENIMAT/i3N, Departamento de Ciência dos Materiais, NOVA School of Science and Technology, Universidade NOVA de Lisboa, 2829-516 Caparica, Portugal; emmanuelle.meunier@casadevelazquez.org (E.M.); esf@fct.unl.pt (E.F.)
3 Casa de Velázquez, EHEHI, 28040 Madrid, Spain
4 Department of Geosciences, Environment and Spatial Planning, Faculty of Sciences, University of Porto, 4169-007 Porto, Portugal; jagoncal@fc.up.pt (J.A.G.); filipa.dias@fc.up.pt (F.D.); allima@fc.up.pt (A.L.)
5 CICGE: Research Centre for Geospatial Sciences, Universidade da Maia—ISMAI, 4475-690 Maia, Portugal; lgseco@ismai.pt
* Correspondence: j.fonte3@exeter.ac.uk

Abstract: Northwest Iberia can be considered as one of the main areas where tin was exploited in antiquity. However, the location of ancient tin mining and metallurgy, their date and the intensity of tin production are still largely uncertain. The scale of mining activity and its socio-economical context have not been truly assessed, nor its evolution over time. With the present study, we intend to present an integrated, multiscale, multisensor and interdisciplinary methodology to tackle this problem. The integration of airborne LiDAR and historic aerial imagery has enabled us to identify and map ancient tin mining remains on the Tinto valley (Viana do Castelo, northern Portugal). The combination with historic mining documentation and literature review allowed us to confirm the impact of modern mining and define the best-preserved ancient mining areas for further archaeological research. After data processing and mapping, subsequent ground-truthing involved field survey and geological sampling that confirmed cassiterite exploitation as the key feature of the mining works. This non-invasive approach is of importance for informing future research and management of these landscapes.

Keywords: airborne LiDAR; aerial imagery; archival documentation; mining archaeology; northwest Iberia; tin

check for updates

Citation: Fonte, J.; Meunier, E.; Gonçalves, J.A.; Dias, F.; Lima, A.; Gonçalves-Seco, L.; Figueiredo, E. An Integrated Remote-Sensing and GIS Approach for Mapping Past Tin Mining Landscapes in Northwest Iberia. *Remote Sens.* **2021**, *13*, 3434. https://doi.org/10.3390/rs13173434

Academic Editor: Antonio Monterroso Checa

Received: 23 July 2021
Accepted: 25 August 2021
Published: 29 August 2021

Publisher's Note: MDPI stays neutral with regard to jurisdictional claims in published maps and institutional affiliations.

Copyright: © 2021 by the authors. Licensee MDPI, Basel, Switzerland. This article is an open access article distributed under the terms and conditions of the Creative Commons Attribution (CC BY) license (https://creativecommons.org/licenses/by/4.0/).

1. Introduction

Northwest Iberia has been long acknowledged as one of the main regions that supplied tin in ancient times [1]. However, archaeological knowledge about ancient tin mining and metallurgy in Northwest Iberia remains very limited [2]. Recent tin and wolfram mines—mainly from the 20th century—may have destroyed previous evidence and the extensive Roman gold mines have been the focus of most of the research.

In Iberian Peninsula, cassiterite occurs in primary (e.g., veins) and secondary deposits (placers and ancient alluviums) [1]. Mining of alluvial deposits involves the excavation of extensive volume of ground, over the entire mineralised area, deeply affecting the landscape, so remote-sensing techniques are very adequate for the research of such areas. Aerial imagery has been used in the past in the Iberian Peninsula, mainly in the context of Roman gold mining, to obtain a comprehensive view of the mining remains and investigate the organisation of mining work phases [3–6]. The use of water-powered technology for the removal of large quantities of sediments, such as ground-sluicing, is responsible for the typical morphology of this kind of vestiges. It became the best-known characteristic of the Roman imperial gold mines, easily observable using aerial imagery. In the last

10 years, airborne LiDAR (light detection and ranging) was also integrated into mining archaeological research, leading to a more detailed understanding of ancient mining areas. Most of these investigations deal with Roman gold mines from Northwest Iberia [7–15]. Regarding tin mining, the study of tin mines in Northeast France stands out [7]. Our approach builds on and complements this previous research, aiming to question the systematic relation between tin mining and the Roman imperial gold mining in Northwest Iberia, an area where tin and gold can occur together in alluvial deposits.

In this framework, the region around the mountain range of Serra d'Arga (Viana do Castelo, northern Portugal), with a high concentration of tin deposit and ancient mining vestiges, is a key area to research, question and integrate common interpretations. For the present study, we selected the sector of the Tinto river valley, a small tributary of the Lima river (Figure 1). It is an area where several ancient mining works have been described in secondary deposits [16–18] and where several recent mining concessions for tin are known [19]. In this work, we developed an integrated study to achieve the first large-scale archaeological map of these mining works, ancient and recent, by combining airborne LiDAR data and archived aerial imagery with geological and historical data. Three following alluvial mining sites in the Tinto valley were selected for detailed analysis using remote-sensing techniques: Sapeiras, Zolas and Rasas.

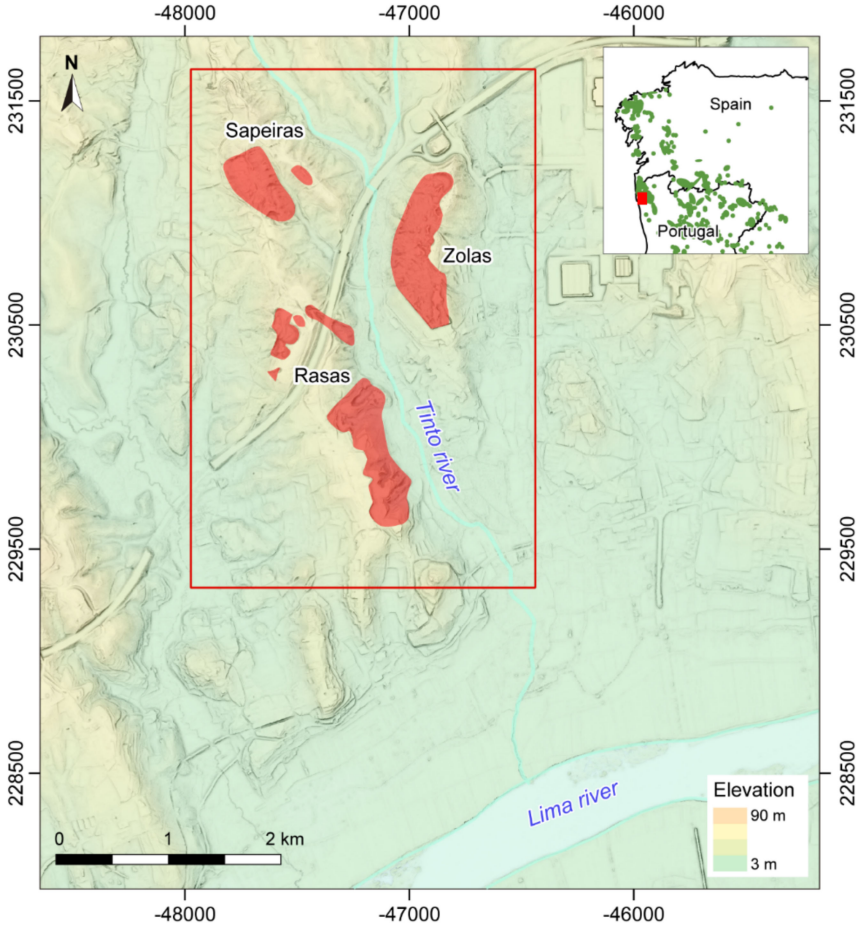

Figure 1. Location of the study area. Mining areas are highlighted in red overlaying light detection and ranging (LiDAR) elevation data. The Northwest Iberia map (right upper corner) gives the location of the study area in relation to tin deposits (green dots) after [2].

2. Materials and Methods

Different types of geospatial data were used and integrated to obtain a representation of the selected mining areas. The airborne LiDAR data were the main data source. To identify the most recent changes in the landscape, archival aerial imagery (from mid-20th

century) was used in combination with older versions of geological and topographical maps and documents from the mining archives (different decades from the 20th century). All geospatial data were projected in the ETRS89/Portugal TM06 (EPSG: 3763) coordinate system.

2.1. Airborne Light Detection and Ranging (LiDAR)

The airborne LiDAR data were provided by the Comunidade Intermunicipal do Alto Minho (CIM Alto Minho). The LiDAR data were acquired between 28 and 31 January 2018, during the off-leaf season, using a Leica ALS80-HP sensor, operated at a laser wavelength of 1064 nm, and an average flight altitude of 2628 masl (meters above sea level) [20,21]. The beam divergence was 0.26 mrad, with a variable pulse frequency between 200 khz and 225 khz, a variable scan frequency between 42 hz and 45 hz, and a variable field of view between 20° and 45°. Up to five return pulses were registered. The entire Viana do Castelo district (Alto Minho region) was flown in 96 strips covering an area of approximately 2260 km^2, which gave an average measuring density of around 2 pulses/m^2 considering only the last returns. The data was distributed in sets of 2 × 2 km^2 LAS files (Figure 2).

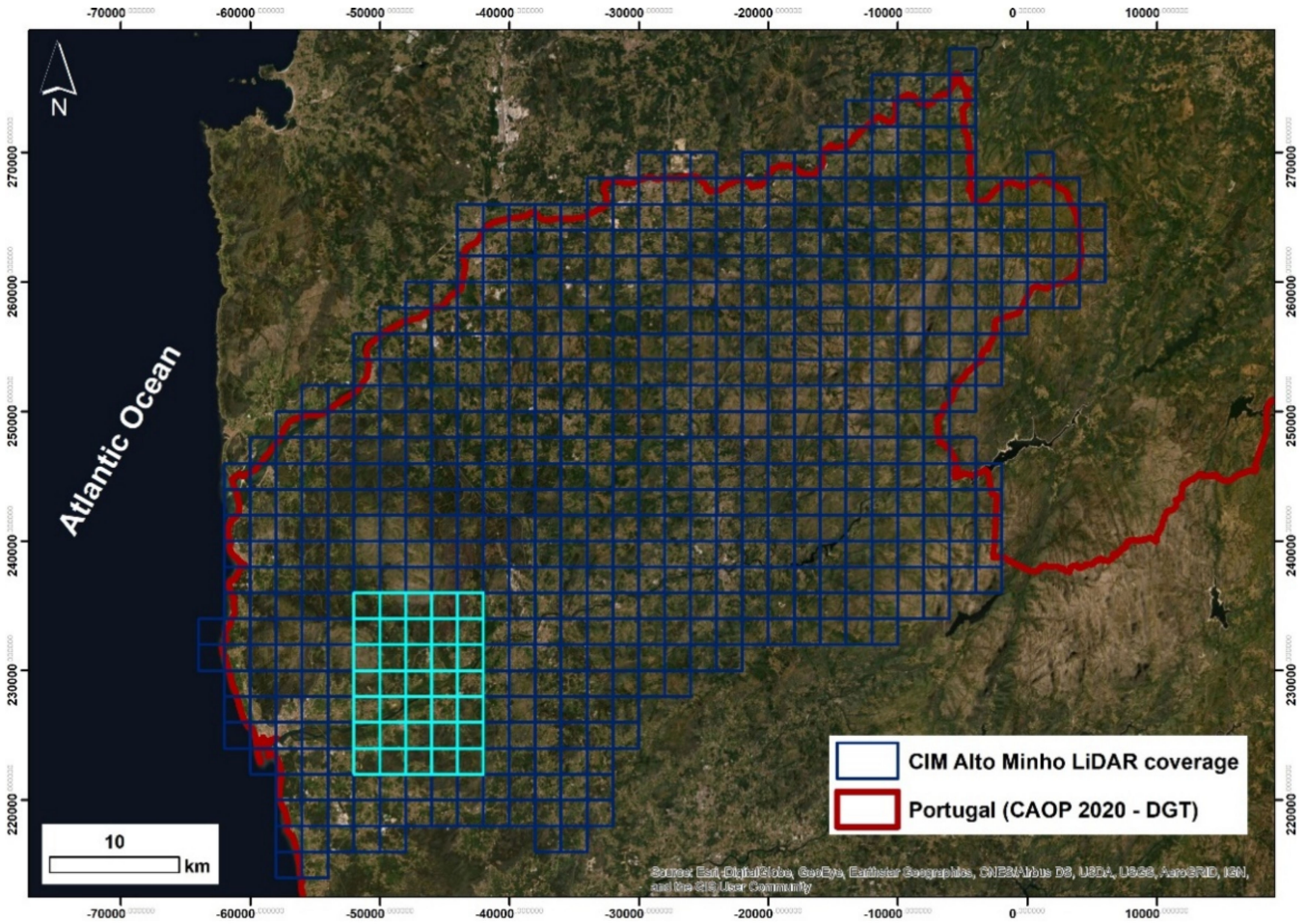

Figure 2. Airborne LiDAR coverage of the Viana do Castelo district (CIM Alto Minho ©), with the study area highlighted in green.

The airborne LiDAR data were processed following a well-documented workflow [22]. A DTM (digital terrain model) with 1 m spatial resolution was generated after automatic point cloud classification. Planlauf/TERRAIN (2021 R1 version) software was used for DTM generation and to extract several visualization techniques, namely a local relief model [23]. The Relief Visualization Toolbox (2.2.1 version) was also used to extract additional visualization techniques from the DTM, namely a hillshade from multiple directions

and a visualization for archaeological topography (VAT) combining hillshade, slope, positive openness and sky-view factor images with parameters adjusted for flat terrain [24,25]. SAGA Wetness Index was also calculated from the LiDAR-derived DTM to highlight the wettest areas and consequently facilitate the identification of the hydraulic infrastructure associated with the mining works [26,27]. Contour lines were extracted every 0.5, 1 or 2 m depending on the relief of each mining sector, using the native QGIS tool. In addition, the QGIS plugin VoGIS-ProfilTool [28] was used to draw topographic profiles of the mining structures, based on the DTM layer, and register their location.

The relatively low-resolution of the LiDAR data, even considering that they were acquired during off-leaf season, meant that in areas of dense vegetation the visualization of archaeological features was more difficult.

2.2. Archival Aerial Imagery

The orthorectification of historical aerial photos is possible by digital photogrammetric procedures [29]. However, frequently the characteristics of the aerial cameras and parameters used in historical photos may not be known, making data processing difficult. A rigorous focal distance and precise coordinates of fiducial marks are examples of such parameters. A solution to overcome this problem is to use the Direct Linear Transformation (DLT) method [30], which was implemented by Pinto et al. [31], due to the absence of stereoscopic coverage. In this method, each photo is georeferenced individually by a rational function, with a total of 11 parameters per photo. This requires at least six control points per photo, normally a few more, to have redundancy. For coverage of several photos, this approach requires a lot of work for ground control point (GCP) collection, which may be difficult for areas with many landscape changes.

A more efficient methodology, described in more detail by Gonçalves [32], applicable to photos with stereoscopic coverage, was used in this work. A similar procedure has already been applied in other cultural heritage-related case studies [33–36]. This makes use of a structure-from-motion approach, allowing for largely automated processing and accounting for camera self-calibration. It also has the advantage of requiring a few GCPs for a full block of aerial photos. The need for fewer points is an important advantage with historical photos because of the many changes in land use and land cover since the time the photos were taken.

This methodology encompasses a pre-processing step where one of the images of a block being processed is chosen as master image. All other images go through an image-to-image registration process to the master image, followed by a resampling, to have the same number of pixels as the master image. This step is done with fiducial marks, which are always present in aerial photos that were acquired for mapping purposes, or any other conspicuous points of the frame. Figure 3 shows two examples of some of the photos used in this project, with different fiducial marks, shown in more detail.

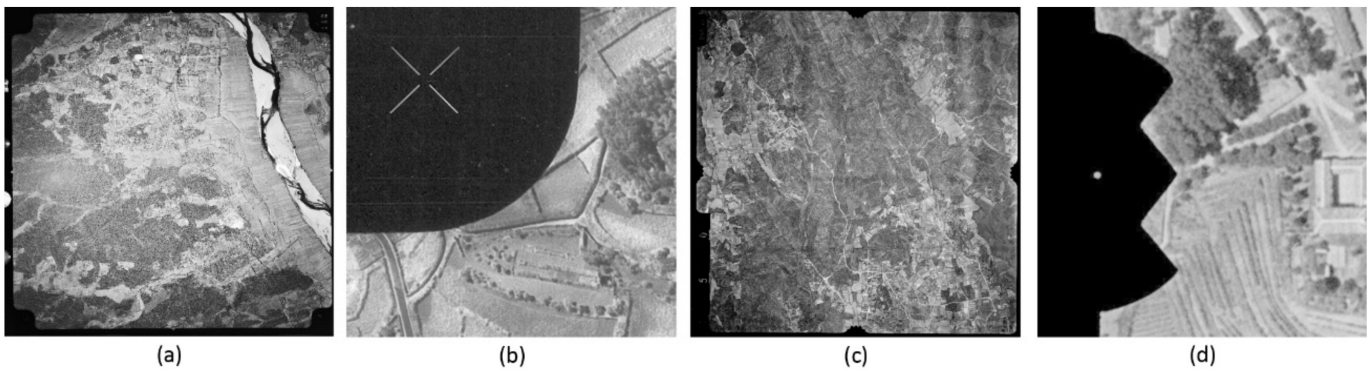

Figure 3. Examples of two photos of different cameras: (**a**) photo with marks in the corners, (**b**) detailed image of corner mark, (**c**) photo with marks on the edges and (**d**) detailed image of edge fiducial mark.

The image-to-image registration process can be undertaken with GIS software. For very large numbers of photos, it might be important to automate this process. However, for the present work, where less than 10 photos per studied area were available, this was done manually. Once all images are registered, they can simulate digital images and be processed in recent photogrammetric software packages, such as Agisoft Metashape, which are normally used for UAV image processing. This program applies structure from motion and multi-view stereo algorithms, largely automated, to derive 3D point clouds, digital surface models and orthomosaics. The only requirements are the pixel size, known from the resolution of the scanner used, and an approximate value of the focal distance, which is normally printed on the images. Even if a precise value is not known, an initial approximate value will be adjusted in the camera self-calibration, together with other relevant camera parameters.

The photos used in this work were provided by the Centro de Informação Geoespacial do Exército and by the Direção Geral do Território (DGT) and were digitized in a photogrammetric scanner. The first Portuguese company of aerial photography, called Sociedade Portuguesa de Levantamentos Aéreos, Lda (SPLAL), acquired the oldest set of photos, as part of a complete coverage of the country made in the decade of the 1940s (1:15,000 scale) [29]. The United States Air Force (USAF) obtained another full coverage of Portugal in 1958 (1:26,000 scale). The third set is more recent, from 1965 (1:15,000 scale), when aerial photography was already common. All were acquired with the standard 60% forward overlap for traditional photogrammetric mapping, using stereoscopy. Table 1 shows details of the images used for three sets of photos: date, number of photos, digitising resolution, and average ground sampling distance (GSD).

Table 1. Data about the image datasets used from Sociedade Portuguesa de Levantamentos Aéreos, Lda (SPAL), United States Air Force (USAF) and Direção Geral do Território (DGT).

Set of Photos	Year	No. of Photos	Scanning Resolution (dpi)	Average GSD (m)
SPLAL	1949	10	1210	0.43
USAF	1958	3	1210	0.59
DGT	1965	4	800	0.58

For the precise georeferencing of the images, GCPs are needed. Although there are good quality geographic data for the area (orthoimages and LiDAR), which would be accurate to provide these points, it was decided to test if this task can be accomplished with Google Earth, since it provides for most of Portugal very high-resolution aerial images. In case of a positive answer, this would justify the generalized use of Google Earth for any other similar studies using historical photographs in Portugal and elsewhere.

Google Earth and Google Maps imagery is traditionally associated with satellite origin, with a positional accuracy of a few meters [37]. Recently, in European countries, orthoimage coverages of aerial photos have been common, following INSPIRE guidelines. They provide a much better resolution and more accurate geolocation. To assess this accuracy, a test was undertaken with 19 well-defined points in the studied area. Coordinates were measured on Google Earth and on the local orthophoto, for the planar coordinates, and on the LiDAR-derived DTM, for the height. Taking these local datasets as ground truth, errors were calculated (E_i) for the n points, as well as the root mean square error (RMSE) according to expression 1.

$$\mathrm{RMSE} = \sqrt{\frac{1}{n}\sum_{i=1}^{n} E_i^2} \quad (1)$$

The values for the three components were:

$$\boldsymbol{RMSE_{Easting}}\textbf{=0.47 } \boldsymbol{m} \quad (2)$$

$$\boldsymbol{RMSE_{Northing}}\textbf{=0.66 } \boldsymbol{m}\textbf{,} \quad (3)$$

$$RMSE_{Height}=0.84\ m \quad (4)$$

These errors are in the order of the ground resolution of the digitised historical photos. Thus, we concluded that in general, Google Earth is an accurate source of GCPs for the georeferencing of historical photos.

Photos were prepared in the way described previously, yielding sets of images all of the same size. After a set of photos was input into Agisoft Metashape (1.7.2 version, Professional Edition), camera data (pixel size and approximate focal distance) was inserted, and the step of image alignment was carried out. In all cases, the method was successful in aligning all images. The following step was the selection of ground control points (GCPs) for the image orientation, which was done using Google Earth, with a total of 8 to 10 points per dataset. Figure 4 shows the 8 points used in the SPLAL image dataset, composed of 10 photos.

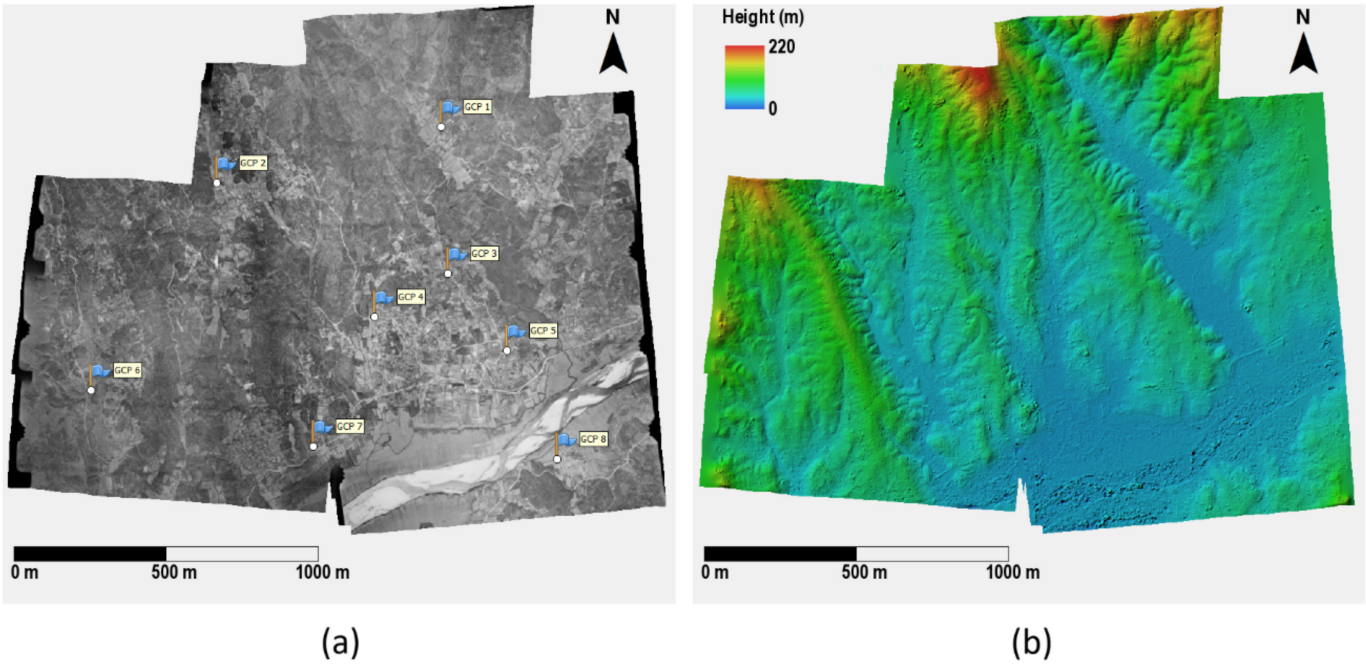

Figure 4. Results of processing the SPLAL dataset: (**a**) Orthomosaic built with 10 photos, with the eight ground control points (GCPs) used; (**b**) digital surface model (DSM) generated, with heights coded in colours and with shaded relief.

The following steps involved the extraction of a dense point cloud, followed by the generation of a digital surface model (DSM). Once the DSM was available, the orthomosaic could be generated. Figure 4 shows the orthomosaic of the SPLAL dataset, and the DSM, with a coloured representation of heights, with hillshading representation.

To assess the quality of the orthoimages, a qualitative assessment compared for several locations the orthoimages produced from the three datasets. Apart from differences of a few meters in the borders of the scene, outside of the area covered by GCPs, there was in general a coincidence within 1 m. The images were also overlaid with accurate GIS data of roads. Figure 5 shows an area with an extension of 800 m, with overlaid roads, for the three orthoimages: (b) SPLAL, (c) USAF and (d) DGT. Image (a) is the SPLAL image without roads. Most of the lines of roads and agricultural paths did not change with respect to the time of images. However, some new roads that did not exist at the time of the images can be detected.

In terms of the assessment of elevation accuracy, a set of 20 points were chosen, within the area covered by the GCPs, in positions with no vegetation and with no clear changes. Heights were assessed in the SPLAL DSM and in the LiDAR DTM. The errors show a maximum absolute value of 3.1 m and an RMSE of 1.42 m. In other conditions, the errors tend to increase, especially outside the GCPs areas, and due to vegetation differences and

other terrain changes. In the case of the other datasets (USAF and DGT), errors tended to be higher due to lower resolution and the lesser number of photos, without lateral overlaps.

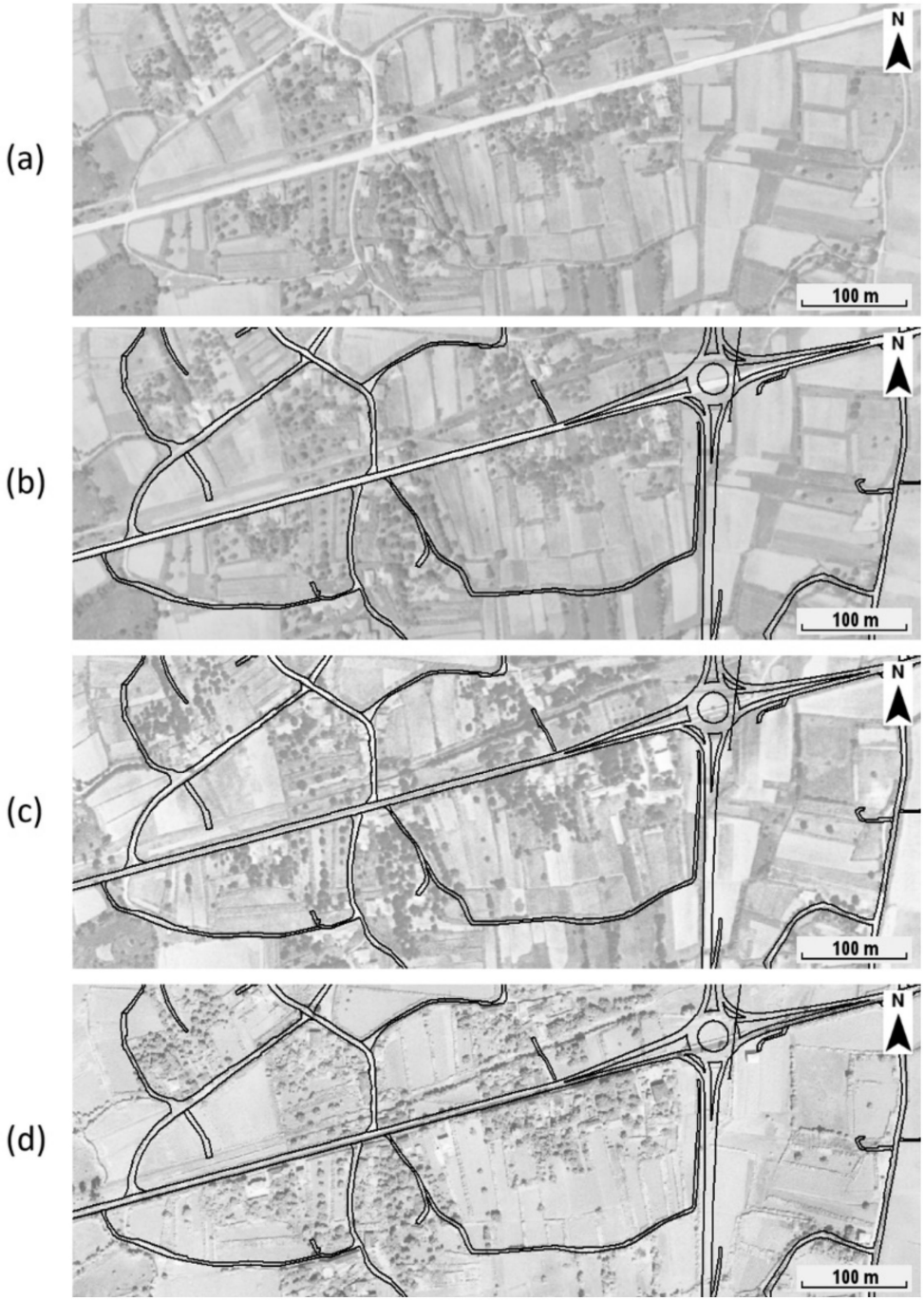

Figure 5. Sample of the three orthomosaics for the selected area with an extension of 800 m to test overlaid GIS data of roads: (**a**) SPLAL (1949) mosaic, (**b**) SPLAL with modern roads, (**c**) USAF (1958) with modern roads, (**d**) DGT (1965) with modern roads. Modern roads derived from the 1:10,000 cartography of the Viana do Castelo Municipality.

Besides the vertical accuracy, of high importance for this work was the capability of extracting topographic details, with high resolution, from the historical photos. Although the DSM generated has a strong noise effect, those areas that are not completely covered with vegetation show very good detail. Figure 6 shows an example of the DSM, in shaded relief form, with overlaid contours of 10 m interval, and the corresponding orthoimage.

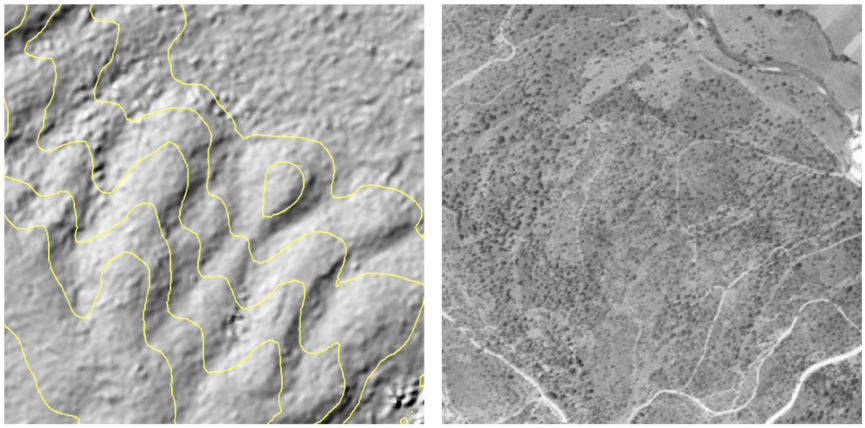

Figure 6. Shaded relief DSM, with overlaid 10-m contours (**a**) and corresponding orthoimage (**b**). The area is a square with sides of 500 m.

Based on this assessment, we conclude that this methodology produces accurate results, both in terms of geolocation accuracy and content, appropriate to integrate with other geospatial data for landscape historical analysis.

2.3. Archival Maps and Documents

In addition to the historical aerial photographs, we used military and geological maps dated up to the year 1949, to confirm the location of ancient paths, roads, or other buildings. They may be unused or destroyed nowadays, but they correspond to alteration of the ground that we must consider in the process of interpreting the LiDAR data. With the same objective, recent aerial imagery (from 1995, 2004 and 2018) made accessible by DGT through Web Map Service (WMS) were used to identify other recent alterations of the ground surface (such as agricultural or forestry activities).

The documents from the mining archives allowed us to confirm if recent mining activity may have overlapped with older structures. These documents are stored at the Arquivo Histórico do Norte do Portugal from the Direção-Geral de Energia e Geologia (DGEG) [38]. Concerning the Viana do Castelo region mining concessions, most of the activity occurred between 1940 and 1960. The documents that brought useful information were the geological and technical reports describing the mining projects, the maps of the concession at scale 1:10,000 and the detailed plans and sections of the mining structures projected, at scales of 1:1000 or 1:2000. In some cases, for underground mining, some plans show the evolution of the works over two or three years. Regarding the opencast mines in alluvium deposits, these archives only included the plans produced for the request of mining permits. The final extension of the mine at the time of cessation has not been registered. All the maps and detailed plans were digitised and georeferenced in GIS to include the location of these recent works in the analysis.

2.4. Geological Sample Collection, Preparation, and Analysis

Fine-grained sediments (mostly between the clay and sand fractions) were collected in the Zolas, Sapeiras and Rasas alluvial deposits by avoiding the places with coarser material. These sediments were washed with a sluice box that conducts the water through itself and separates the sediments by density. The denser sediments that became trapped in the sluice box were then panned to improve the separation process needed to concentrate the cassiterite. The concentrates of the denser sediments were analysed with a portable X-ray fluorescence equipment (pXRF) (Bruker S1 Titan 600, with a rhodium anode, a maximum power of 2 W, a cathode potential of 15–50 kV and a current intensity of 5–100 μA). Each analysis had a duration of 90 s, and three to four shots were fired in each sample, being considered the average values.

Four sets of panned samples were analysed for the three studied areas. Rasas had two visually distinct types of material inside its alluvial deposits (an altered white material and an orange clay) and, therefore, samples from both were collected. The panned sediments from Sapeiras and from the Rasas (clay) gave low Sn contents, therefore, to confirm the presence of cassiterite in these sediments they were further separated using optical methods.

The results of the elemental analysis are presented in Tables 2 and 3.

Table 2. Qualitative chemical analysis from the portable X-Ray fluorescence (pXRF) equipment in the panned samples collected from alluvial deposits in Sapeiras, Rasas and Zolas. In Rasas, two different fractions of sediments were analysed, one constituted by altered pegmatite (peg) and the other by an orange clay (clay). The results are an average of at least three analyses for each sample.

Element (%)	Sapeiras Panned Sediments	Rasas (Peg) Panned Sediments	Rasas (Clay) Panned Sediments	Zolas Panned Sediments
Sn	0.07	0.35	0.19	0.32
Fe	0.68	0.33	2.14	2.03
SiO_2	48.4	47.3	33.9	2.01
Mn	0.03	0.20	0.66	-
Nb	0.01	0.11	-	0.05
Ta	-	0.06	-	-
Zr	0.12	0.01	-	0.07
Zn	0.06	-	0.06	0.02
Ti	0.69	-	0.07	0.12
Pb	-	-	0.06	-
V	-	-	-	0.02
K_2O	0.26	0.98	0.52	0.11
Ba	-	-	0.14	-
Rb	-	0.02	-	<0.01
Al_2O_3	1.21	5.41	2.77	
S	0.04	-	-	-
Ca	-	0.02	-	-
Hf	<0.01	-	-	-

Table 3. Qualitative chemical analysis from the portable X-Ray fluorescence (pXRF) equipment in selected grains from the panned samples collected from the alluvial deposits in Sapeiras and Rasas. In Rasas, two different fractions of sediments were analysed, one constituted by altered pegmatite (peg) and the other by an orange clay (clay). The results are an average of at least three analyses for each sample.

Element (%)	Sapeiras Selected Grains	Rasas (Peg) Selected Grains	Rasas (Clay) Selected Grains
Sn	15.4	11.8	11.8
Fe	1.52	0.91	12.2
SiO_2	1.16	3.22	1.63
Mn	0.01	4.83	3.57
Nb	0.15	0.06	0.09
Ta	-	-	0.13
Zr	0.01	-	<0.01
Zn	4.18	1.25	0.05
Cu	0.01	0.12	-
Pb	-	0.31	0.34
Ga	0.03	-	-
K_2O	-	0.15	0.17
Ba	-	0.69	0.65
Rb	-	0.01	0.02
Co	-	0.22	-
Sr	-	-	0.01

The calibration method chosen for the first analysis was the "Geoexploration" due to the low Sn concentrations on the panned sediments. The analysis of these sediments revealed Sn at concentrations of 0.07–0.35% (qualitative analysis, Table 2), which suggested the presence of cassiterite. However, to confirm the presence of cassiterite a gemologist loupe was first used and then a stereo zoom microscope, to select cassiterite-like grains and to analysed them again (Figure 7). The "Geomining" calibration was then chosen for the following analysis since it is more accurate for high concentrations of ore metals such as Sn, Fe and Au. The analysis of the selected grains (Table 3) indicated Sn concentrations of 11.8–15.4 % (qualitative analysis, Table 3), which confirmed the presence of cassiterite (note that the values result from using default calibrations of the equipment).

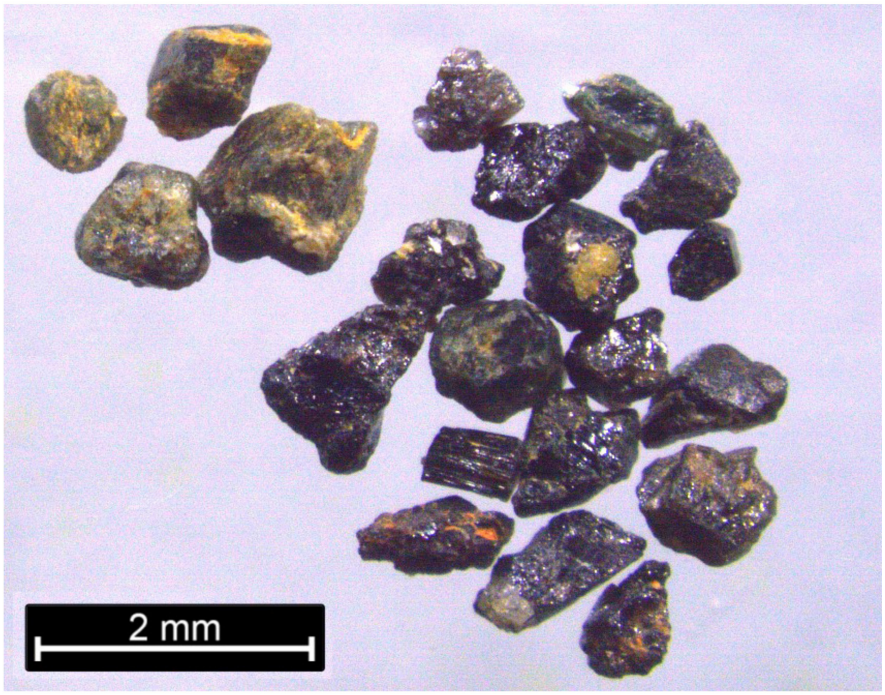

Figure 7. Microphotograph of some grains separated with the gemmologist loupe from fine grain sediments taken at Sapeiras mine. Most of the cassiterite grains are on the centre and right side of the image.

3. Geological Context

The Rasas, Sapeiras and Zolas mining areas are within the tectonostratigraphic area of Galicia and Trás-os-Montes Zone (GTMZ) (Figure 8). These areas are located on old quaternary terraces, classified as T2 according to Caetano Alves [39], from the Middle Pleistocene epoch. The terraces are the result of an exoreic drainage system that formed the current river drainage systems and are part of the Lima river main catchment basin. They are cut by some tributaries, such as the Tinto river, the Seixo river, the Areeiro river and the Sapeiras river. The Lima terraces have been classified into four types (T1, T2, T3 and T4), with T1 being the oldest and T4 the most recent.

Each new terrace represents a new process of erosion of the local lithologies and a new sedimentation [39,40]. Thus, the material found on the terraces is controlled by the bedrock composition.

The geological sample collection was collected at T2 terraces. The T2 terraces are upon mica schists from the metasediments constituting the Central and Western Minho Unit (CMU), within the GTMZ. These metasediments from Viana do Castelo region contain important mineral resources with the following decreasing order of importance: tin (Sn), niobium (Nb), tantalum (Ta) in pegmatite veins and alluviums, and tungsten (W) and gold (Au) in quartz veins [41].

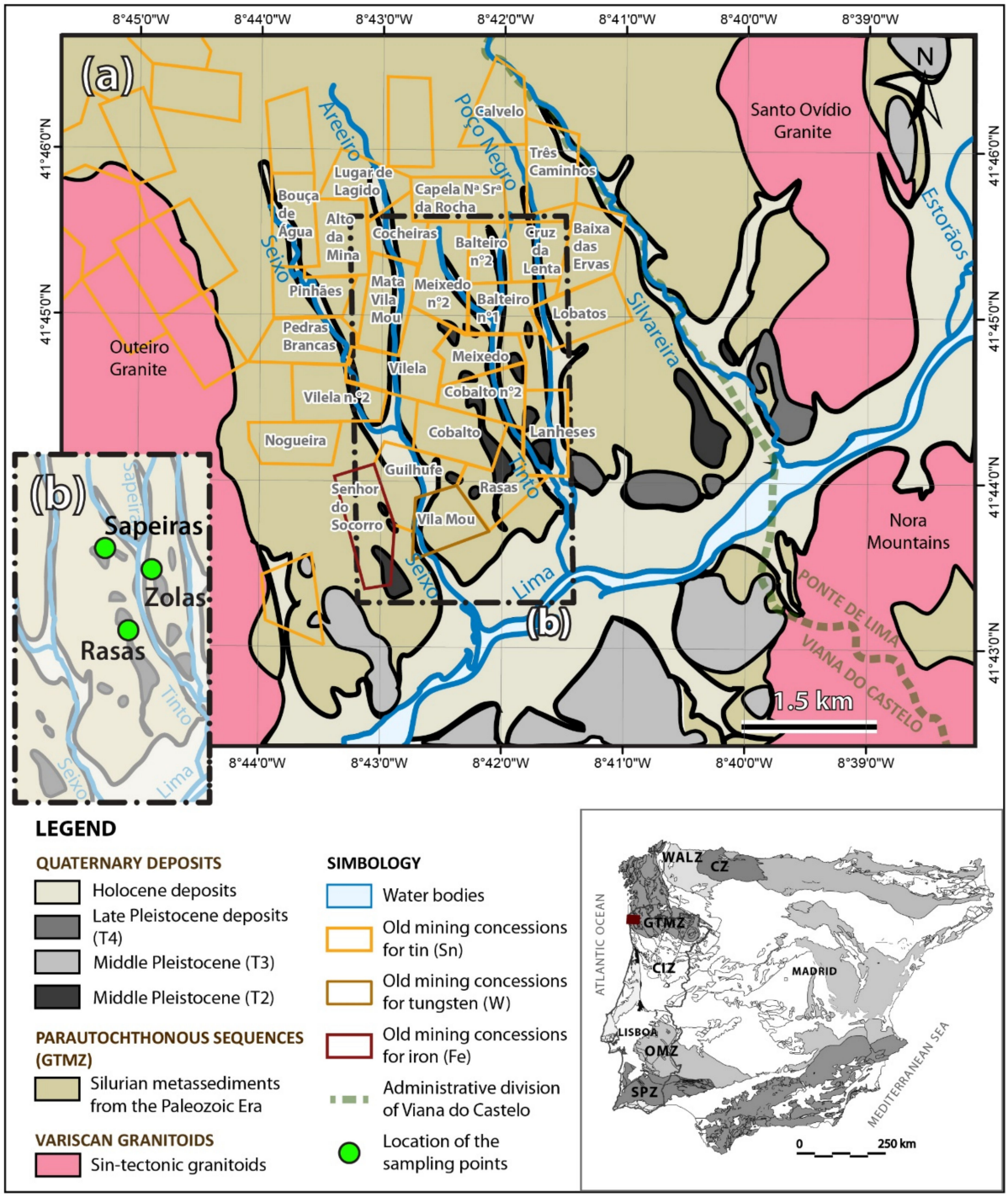

Figure 8. Geological map of the Lima river catchment basin with its Cenozoic sedimentation (adapted from [42]) with (**a**) the mining concessions of the 20th-century [19] in the municipality of Viana do Castelo (depicted as old mining concessions) and (**b**) location of the sampling points for Sapeiras, Zolas and Rasas which are over T2 old terraces [43].

In the T2 terraces, it is common to find goethitic crusts (layers of iron oxide with a reddish-brown colour mixed with pebbles from conglomeratic zones), often at the bottom of the terraces, in the contact zone with the kaolinized mica schists. These terraces are found at an altitude between +40 and +50 m (never reaching the 70 m) and their thickness may change from a couple of meters to almost 15 m according to the local geomorphic setting and palaeochannel morphology [39,44].

The T1, T2 and T3 terraces are described as having essentially a siliceous composition ($\geq$90%), mainly constituted by coarse clasts, where 80% is normally quartz. They also

have a finer fraction, sand dimension, that mostly consists of quartz, micas, tourmaline, andalusite and some zircon, titanium oxides, cassiterite and staurolite. In lesser quantities, there is an even finer fraction, basically clay, usually constituted by kaolinite, illite and goethite [39].

The area of the municipality of Viana do Castelo was extensively mined for tin (Sn) in the 20th century, by extracting it from cassiterites (SnO2), mainly from pegmatite veins and alluviums [41,45]. Rasas, Sapeiras and Zolas are in an area full of abandoned Sn mining concessions (Figures 8 and 9). The Cruz de Lenta, the Meixedo and the Cobalto n.º2 mining concessions, surrounding the Poço Negro river and the Sapeiras river, were Sn concessions described as having alluvial deposits consisting of rolled pebbles and ferruginous clay, mineralized by cassiterite, with an average grade from 2 kg/t to 2.5 kg/t. In addition to cassiterite, the only other mineral regarded as having some possible economic interest (mentioned in the reports from the mining concessions) was very fine tantalite (<2 mm) and only in small quantities [46–48]. Regarding gold, we cannot totally exclude that it could have been exploited in these alluvial deposits in ancient times (Iron Age or Roman period). However, all geological data indicate that cassiterite was the main mineral, so gold would have only been a secondary product of these mines at the best.

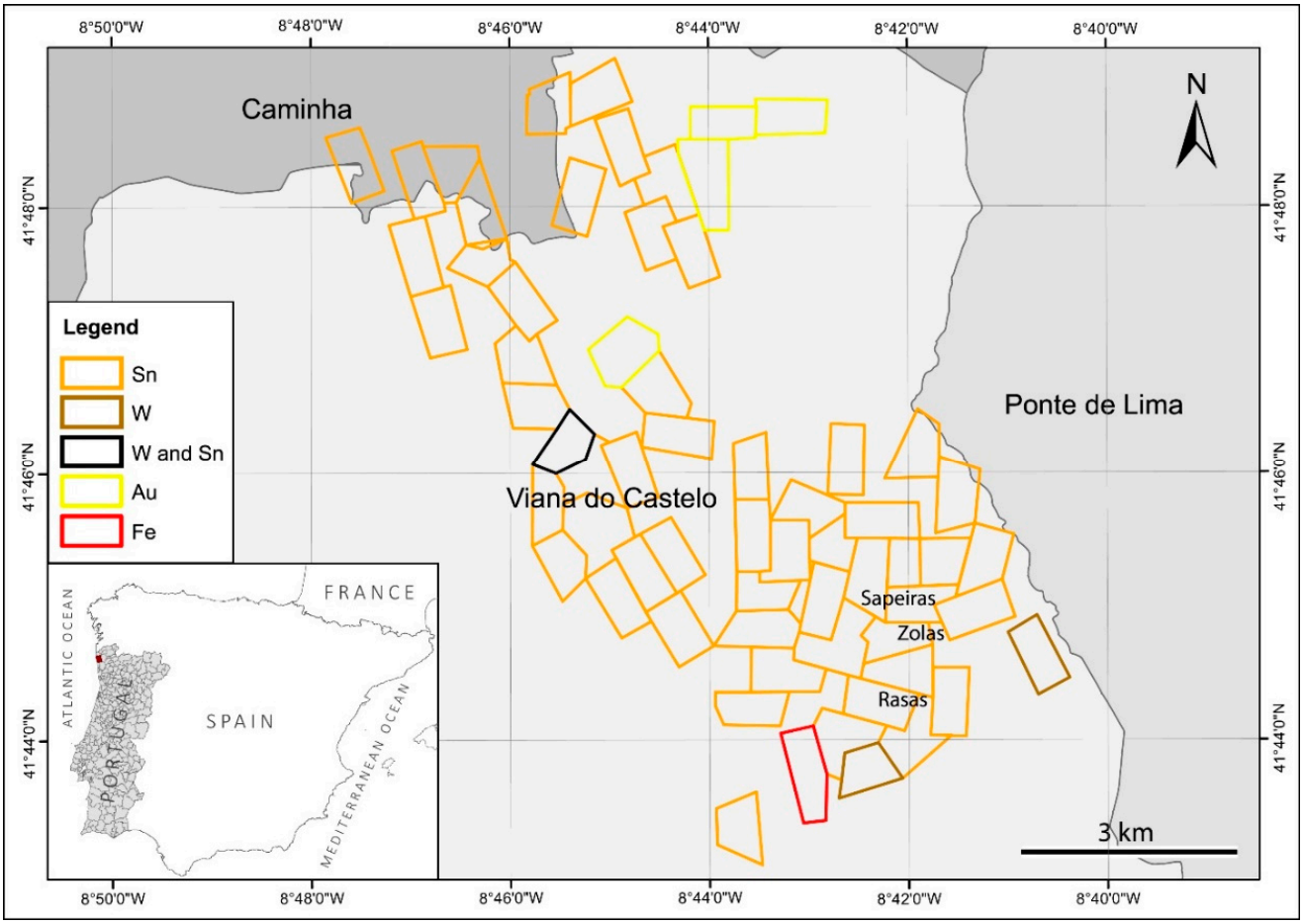

Figure 9. Viana do Castelo municipality and its mining concessions. Data retrieved from the DREN (Direção Regional da Economia do Norte) archives and [19].

4. Results

4.1. Characterisation of Modern Mining According to the Documentation of Mining Archives

During the 20th century, mining concessions in the Rio Tinto area focused mainly in mining alluvium and in some cases veins, materialized in many opencasts and some underground works. Regarding alluvium, the documents available in the archives indicate

that the areas of interest were, during the 1950s, those along the many watercourses of the area. The method of mining was, therefore, designed to preserve the land for agriculture or livestock farming during and after the end of exploitation. The ground was divided into quadrangular sections where organic soil was extracted and stored apart. The mineralized levels below were extracted and processed in washeries close to the pit. The barren sediments were placed back into the trenches and covered again with the organic soil previously separated (Figure 10). This type of mining left no trace in the landscape after a few years, when the vegetation grew again.

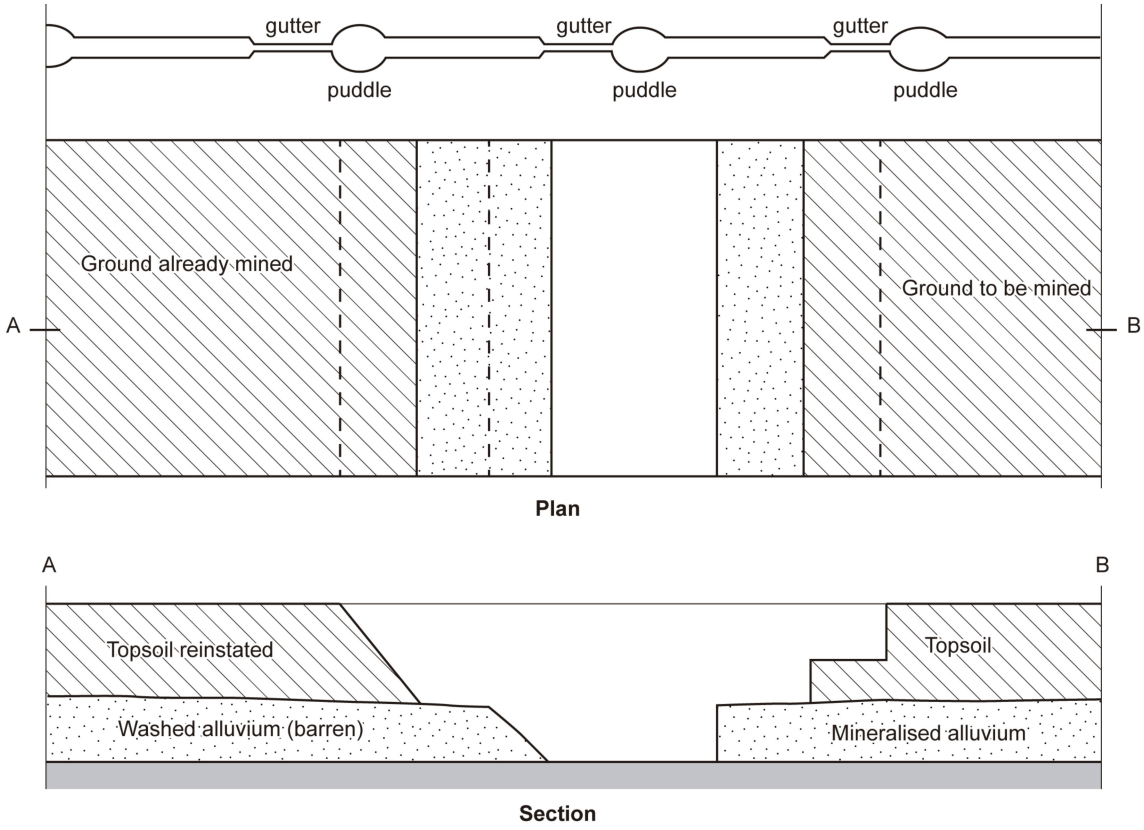

Figure 10. Scheme of alluvium mining based in projects dated between 1940 and 1960 (adapted from [48]). Topsoil is typically within 1.5 to 2.5 m thick.

The reports of mining engineers also mention the frequent presence of superficial diggings done by local people a few decades before, carried out with limited means. This kind of illegal mining was very frequent during long periods of the 20th century, mainly during World Wars I and II. The location of theses diggings such as their real extension is never reported. Despite this, older diggings cannot be excluded. 20th-century mining diggings could of course locally disturb archaeological features, but as these type of works had small extensions and did not go deep, their impact was probably quite reduced. In general, there is no indication of archaeological evidence in these reports. The only exception is in the Alto da Bouça da Breia mine, to the north of Viana do Castelo municipality. There, the reports mention old underground galleries along a quartz vein with gold and opencast trenches along aplitic veins with tin, supposed to be from the Roman period [49], but with no possibility of access nowadays. Our integrated approach shows that archaeological mining remains can also be present and recognised in some secondary mining deposits.

4.2. Mapping of Mining Works

By combining several LiDAR-derived visualizations (Figure 11), we first defined the limits of the different mining areas identified (Sapeiras, Zolas and Rasas), as well as part of

their internal structures: mining trenches, water channels, water tanks, area of rejection of sterile sediments. The possibility of drawing such elements was strongly dependent on the resolution of LiDAR data and the vegetation coverage. The other data sources were used as complements of LiDAR data. Special attention was put on identifying the ground cuts or areas where a first hollow was made and afterwards deepened. These elements helped to define a relative chronology of the structures superimposed to others. Another essential element was the direction of the slope in each sub-sector of the mining areas, being the DTM and contour lines the most helpful for that task. Slope analysis is essential to assess the possible use of water-powered technology such as ground-sluicing and to understand the organisation and work progression of the mines. The areas affected by recent ground modifications were also highlighted in our mapping, using the 1:10,000 vector cartography of Viana do Castelo and drawing old paths, roads, or other structures visible in aerial images.

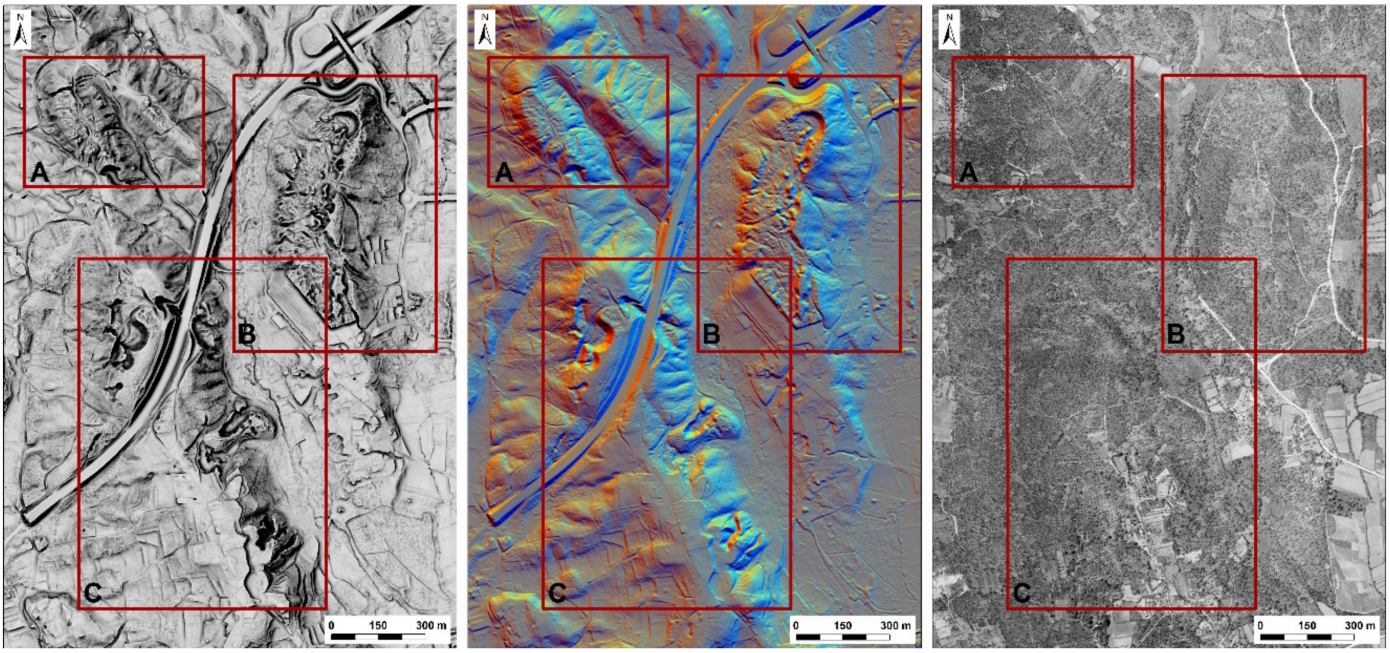

Figure 11. Mining areas overlapping (from left to right) VAT (visualization for archaeological topography), hillshade from multiple directions and SPLAL orthoimage: (**A**) Sapeiras, (**B**) Zolas and (**C**) Rasas.

In order to confirm the mapping and interpretation of LiDAR-derived visualizations, a ground-truthing campaign was carried out, consisting of a surface survey in all areas where vegetation allowed it. Field photos of the more significant structures were taken to complete the recording.

The mining structures identified include mainly opencast works in the upper alluvium terraces. The fact that the activity in the frame of the mining concessions focused on the lower terraces, along the watercourses, confirms that the structures visible in the LiDAR data are older. The overall forest cover in Sapeiras, Zolas and Rasas areas visible in the SPLAL 1949 orthoimage (but also in the USAF 1958 and DGT 1965 images) confirms that there was not active mining works in that places at that time, which would have implied the deforestation of the area.

4.2.1. Sapeiras

The Sapeiras mine includes clear vestiges of the 20th-century mining to the north (Figure 12). They include a series of pits cutting the bedrock over more than 250 m in length. These structures are clearly visible in the aerial photograph of 1949, showing that they were excavated quite recently. In the 1958 photographs, the trees have nearly completely covered them, and it is no longer possible to see them in the 1965 set. The project of 1954

for the Meixedo 2 concession refers to this opencast mining, as works upon an aplitic vein, subvertical, mineralised with cassiterite, embedded in schists. It includes a proposal for the extension of underground works, up to 68 m in depth. The fact that no signs of such work are visible in the 1958 pictures let us think that this project did not have an important development. This project also included a proposal for alluvium mining along the small watercourse in the middle of this area. No pit is visible in the 1958 orthoimage, but the ground along the watercourse is clear of trees and this might be related to vegetation clearance due to the mining activity.

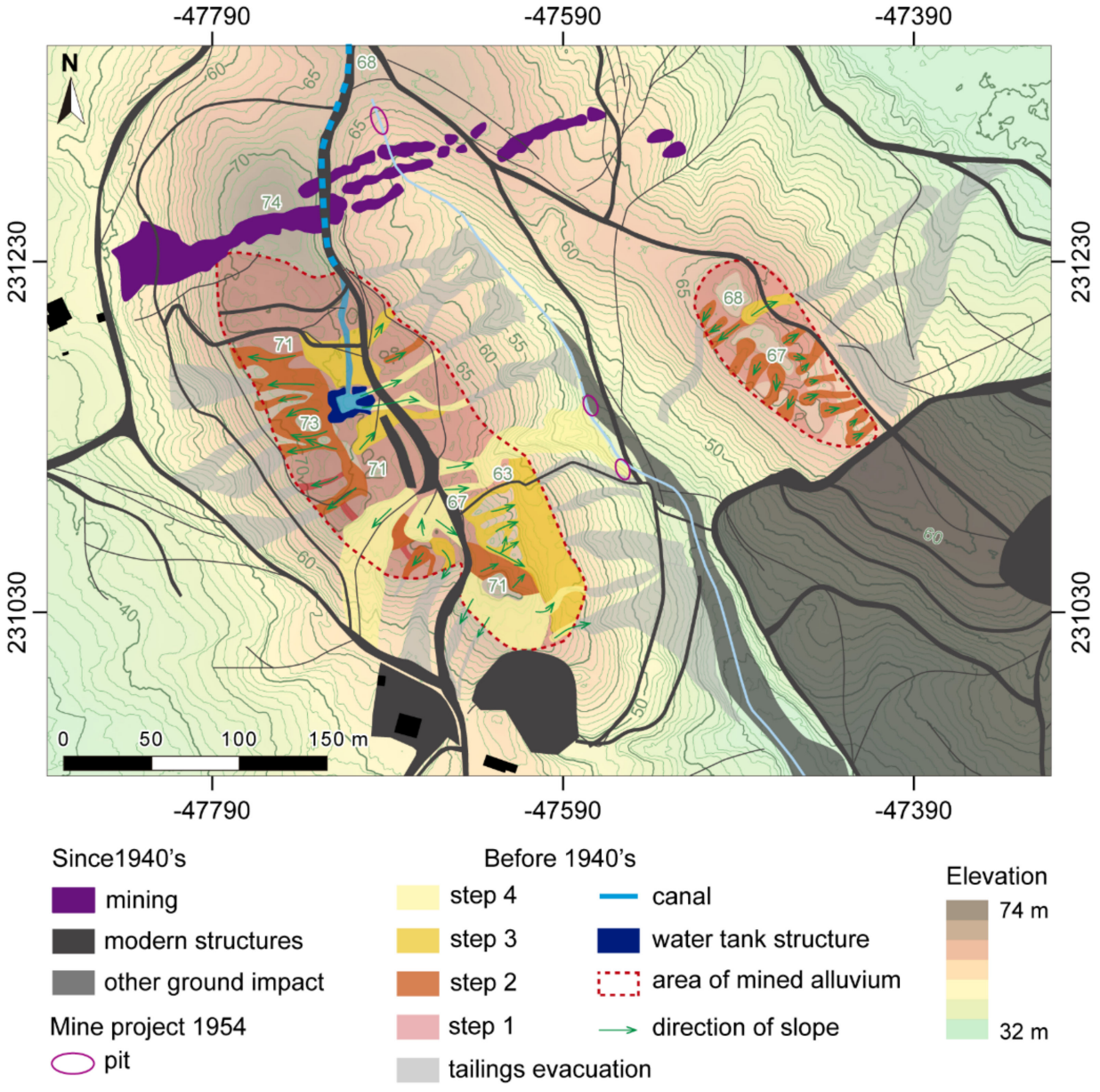

Figure 12. Mapping of Sapeiras mine, with indication of recent structures (constructed since 1940) and relative chronology of older features (step 1 being the oldest). Structures related to hydraulic features are highlighted in blue.

In Sapeiras two ancient mining sectors can be identified: the largest in the west and a smaller one in the east, both at the top of ridges. The mining of the upper alluvium resulted in a flattened area in the western sector and in a more irregular succession of trenches and mounds in the eastern one (see in Figure 13A,B). The trenches on the slopes correspond to the evacuation of the tailings, but some others, larger and deeper, could correspond to the mining of the lower part of the terrace.

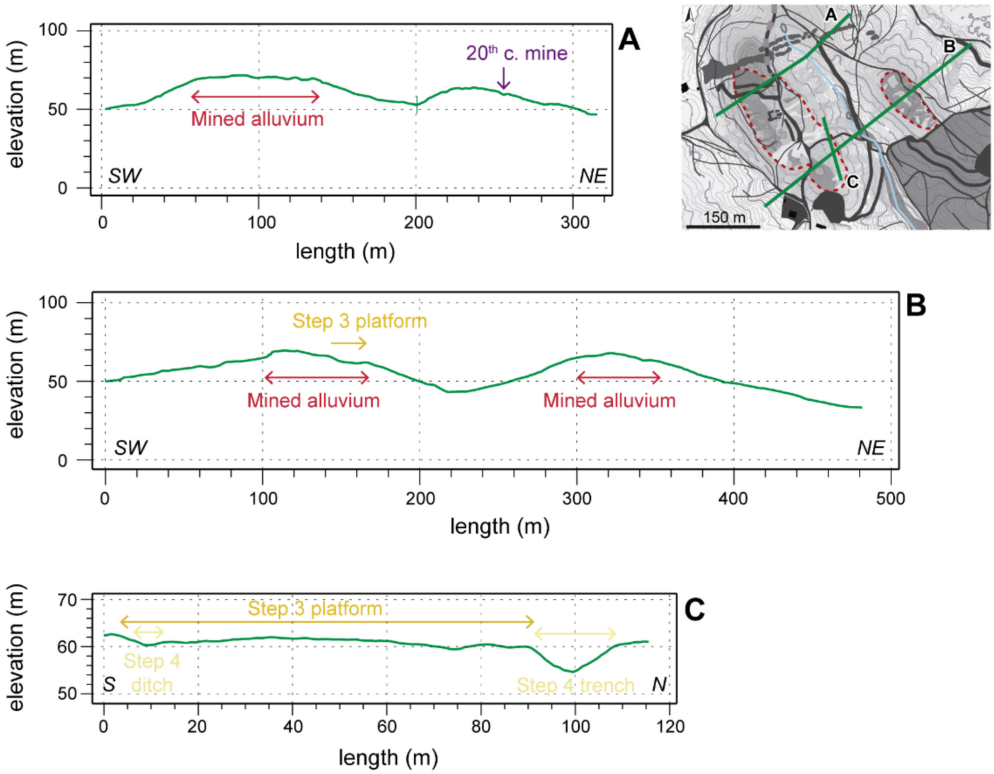

Figure 13. (**A**–**C**) sections of Sapeiras mine.

The eastern sector has a simple structure: mining trenches are located on each side, following the natural slope. In the western sector, the interruptions and deepening of the different structures make us propose four steps of mining. Step one, the oldest one, resulted in a first flattening of the upper part of the ridges. The vegetation and the changes resulting from the following steps do not allow us to describe in detail the organisation of this first mining phase. However, the mounds and depressions confirm that the ground was subject of mining. Step 2 is defined by a series of trenches directed to the slopes. Steps 3 and 4 resulted in larger and deeper excavations, on the top of the ridge for step 3 and along the slopes for step 4.

We notice the excavation of a very regular platform in the southeast part of the western sector, during step 3 (Figure 13B,C). It is around 100 m in length, 20 m in width and the ground was removed to a thickness of 5 m. This structure is nearly completely hidden by the trees in the field and would not have been recognised without the LiDAR data.

Another interesting structure is the small water tank in the centre of this sector (Figures 12 and 14). It is not clear on the LiDAR data and unrecognisable on the historical imagery, but the prospection on the ground allowed us to confirm its nature. It is a rectangular hollow (9×11 m^2) delimited by an embankment (20×24 m^2) with two exit channels on its eastern side and a small depression in the north side of the embankment, that would correspond to the water inlet. Even at the time of prospection during mid-summer, the centre of the structure was wetter than the neighbouring ground. Only the modern road interrupts the exit channels, so the structure must belong to the last phase of ancient mining. This road, following the line of highest elevation in the north, must have been reused and then destroyed the duct supplying water for this small tank. Similar structures are not reported in the literature for ancient alluvium mining in northwest Iberia. The water tanks described are located in the periphery of the mines and have larger dimensions, up to 100 m, as reported in [50]. This one, much smaller and inside the mine, could not have been not designed to remove very high volumes of sediment: both exit channels are quite narrow and do not create large excavations. With this configuration, we can propose that it was used for a last attempt to mine the terrace, at a small scale, or to

wash sediments excavated close to it and so separate the cassiterite from the barren clay. An excavation of the structure would be necessary to confirm this hypothesis.

Figure 14. Sapeiras mine. View of the water tank, from the west.

4.2.2. Zolas

The Zolas mine, on a small hill, is preserved along 700 m from north to south and around 150 m from west to east, with no interruptions of the mining structures. It is the more extended ancient alluvium mine of Viana do Castelo. The impact of recent structures is relatively significant, with a dense path network and a large area excavated and flattened to the south, cutting the mining vestiges (Figure 15). The mining project of 1953 for the Meixedo 1 concession included some pits for alluvium mining close to the small watercourse to the west, out of the ancient mining area. To the north of the mine, the motorway makes it difficult to perceive the landform, but it is possible to observe a gentle depression in that direction, going down to 49 m. Considering that the mining vestiges cut the ground at 60 m at the highest (Figures 15 and 16), this is an issue regarding the potential use of hydraulic systems to mine these alluviums. The closest watercourses flow 30 to 40 m lower than the highest part of the mine.

The ancient mining remains are mainly on the western slope of this small hill, where the ground was removed up to 10 m in depth (Figure 16A,B). To the south, a small area on the eastern slope was also mined and the ground removed up to a thickness of 5 m (Figure 15B). The mined area could be described as a roughly horizontal artificial platform. Some trenches in the slopes correspond to the evacuation of tailings (Figure 15). The dense vegetation does not allow us to propose a precise mapping of the internal trenches of this mine. However, four mining stages could be defined. This proposal might be reviewed in the event of a future micro-topographic survey after the deforestation of the area.

Figure 15. Mapping of Zolas mine with indication of recent structures (constructed since 1940) and relative chronology of older features (step 1 being the oldest). Structures related to hydraulic features are highlighted in blue.

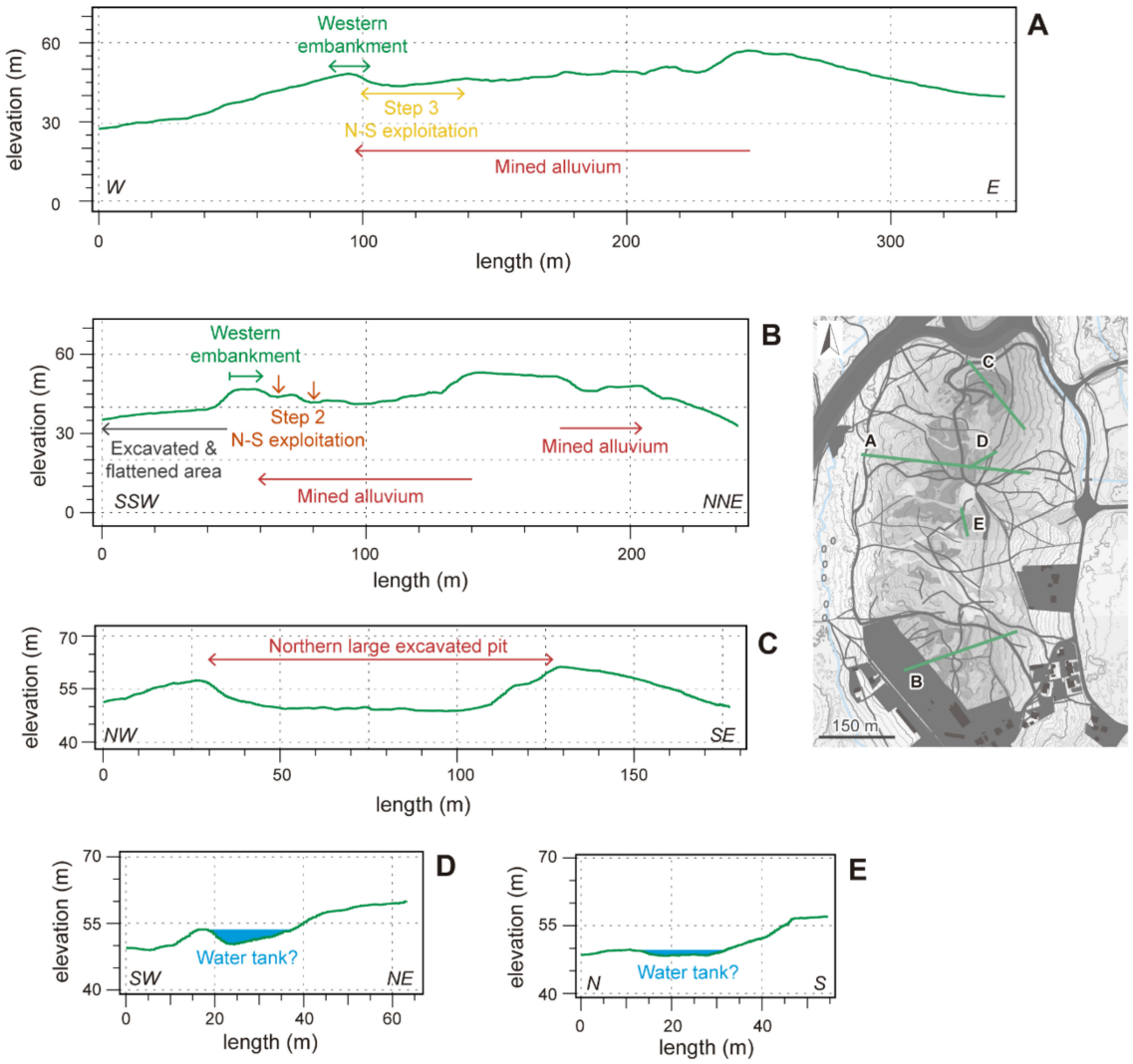

Figure 16. (**A**–**E**) sections of Zolas mine.

In most of the mine, mining was conducted from the east to the west, following the natural slope. This general frame was, however, modified in some places, as a small embankment (from 1.5 to 4 m high) appears on the western side of the mine (Figure 15, green dot line and Figure 16A,B). In other places, changes in slope orientation helped differentiate the mining phases and highlight the eastward orientation of some trenches of the last period of activity. However, in some cases, this draws small, enclosed structures of 20 to 25 m in diameter and 1.5 to 2.5 m in depth, where some water could remain (Figures 15 and 16D,E). We propose that these structures could correspond to small water tanks. To confirm this, an excavation would be necessary to observe the geomorphological characteristics of their filling and their internal structure. The vegetation is now too dense to ground truth it. Their size, as in the case of Sapeiras, is too small to consider that they were key structures of the main digging work. Anyway, the need for washing the sediments to separate the cassiterite from the clay required the presence of water that could have been at least partially covered by this kind of structure. However, the question of the origin of the water to fill them is unsolved, as no remains of ducts are visible nowadays in this mine.

Despite the difficulty to map in detail many parts of the mine, we can distinguish the trenches, rather long and narrow, from other bigger structures with more roughly circular shapes that we could describe as some artificial large excavated pits (Figures 16C and 17). The trenches are present all over the mine, as shown by LiDAR data, whereas the bigger

structures are located only along the highest part of the ridge. They represent two different ways of conducting the mine, adapted to the thickness of the mineralised terrains.

Figure 17. Northern large excavated pit of Zolas mine, seen from the south. The 10 m distance lines mark the depth of the pit.

4.2.3. Rasas

The Rasas mine is formed by several structures along a small ridge, mainly on its eastern slope but with a few of them on the western one, to the north of the mine. In addition to the motorway passing close, the houses and the road in the upper part of the ridge, and the numerous paths in the slopes, affected the ground in diverse ways. This mine is partly in the modern concession of Cobalto 2 where some pits for alluvium tin mining were planned in 1953. As we can see in Figure 18, they could affect the extremity of one of the ancient mining structures. Precisely at the lower part of this large trench, the presence of abundant slag and some remains of furnaces were reported by Moreira [17] (pp. 406–407), who considered them as archaeological traces from the Roman period and not from the 1950s activity, but without clear chronological data. He gives no indication of recent mining in this specific place. We do not know if it is due to the careful reinstatement of sediments as specified in the scheme for alluvium mining at the region (Figure 10), or because the mining project was never developed. In fact, no mining pits are visible in the aerial images of 1958. In the field, we could not examine in detail the lower part of the large trench, full of dense vegetation. We were, however, able to find small concentrations of iron slag, of unknown chronology.

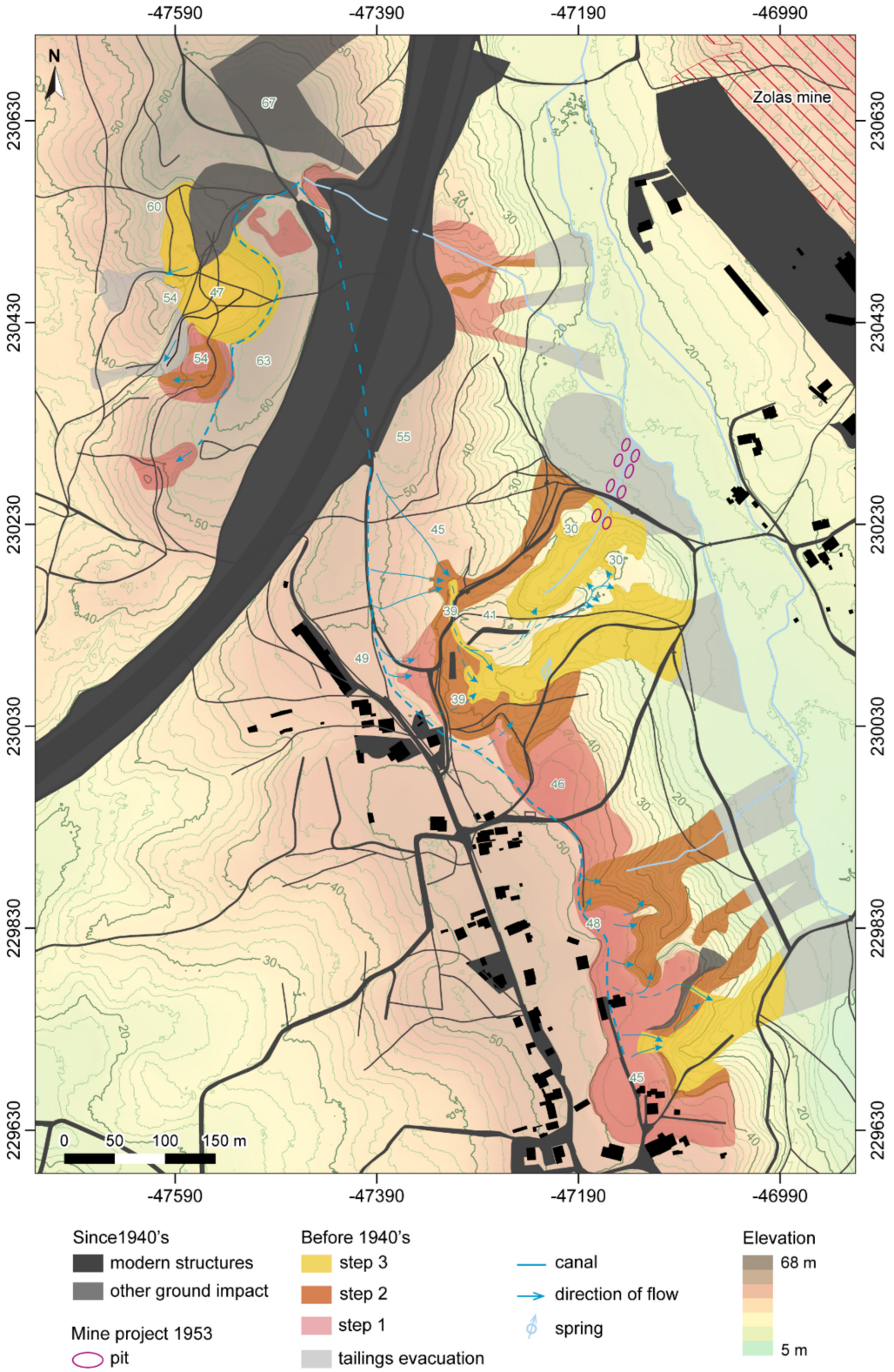

Figure 18. Mapping of Rasas mine with indication of recent structures (constructed since 1940) and relative chronology of older features (step 1 being the oldest). Structures related to hydraulic features are highlighted in blue.

Regarding the ancient mining structures at Rasas, their organisation is simple. We can observe some large excavations on the slopes, each independent from the others. Some breaks in the upper part or at the borders of these excavations (Figure 19A–C) indicate

distinct phases of mining, with the deepening of the mine. To the north, a small area could have been superficially mined in the upper part, as some irregularities in the ground seem to indicate. In the southern part, connecting the large structures on the slope, a roughly horizontal elongated area, delimited by an embankment in the west, could correspond to the first step of mining. The ground appears to have been flattened around the elevation of 46 to 45 m, forming a kind of platform that does not exist on the natural slope on the west (Figure 19B,C). This type of excavation following a certain elevation can be compared with the Zolas mine or with the long platform in Sapeiras mine.

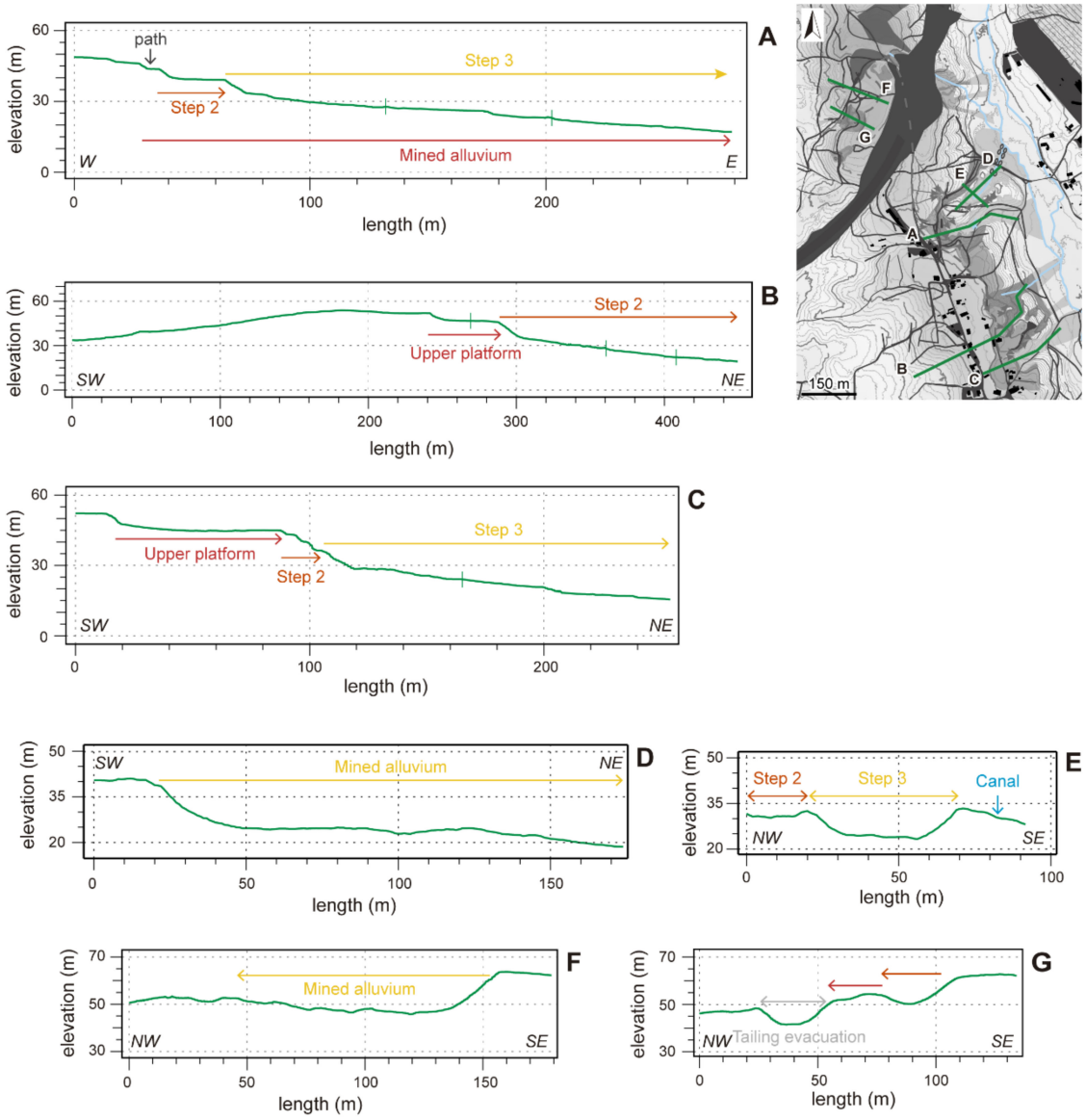

Figure 19. (**A**–**G**) sections of Rasas mine.

On the slopes, the excavations are large and deep. Most of the mining structures are elongated in plan, sinuous in some cases, and range from 25 to 50 m in width and from 6 to 10 m in depth (Figure 19A–E). We also observe two large excavated pits in the north, comparable with the largest of Zolas mine, of 50 and 100 m in diameter and 9 to 16 m in depth (Figure 19F,G). A deep trench allowed the evacuation of tailings for both. The volume of sediment removed and processed in the whole mine must have produced a large amount of waste. The small valley to the east of Rasas mine was quite certainly strongly impacted by the accumulation of tailings, even if the small river contributed to transporting them south to the Lima river.

The last element that we want to highlight in this mine is that three small watercourses flow in three of the mining structures and a spring is present in a fourth one (Figure 18), showing that obtaining water for mining there was probably not a problem. It is possible in this case to reconstruct the water network used for mining, with a starting point in the north, where a watercourse springs at an elevation of 61 m. This point coincides with the highest level of mining. We can suppose that two main channels drove the water to the eastern and western mining structures. In the western side, the upper limit of the large excavated pits were 10 m westward according to the 1949 photographs when compared with the LiDAR data. We can suppose that erosive processes led to the destruction of the water canal in the upper part, which had to pass quite close to the limit of the mine, considering the elevation of the spring. For the eastern slope, the wide cut in the ground made for the motorway (15 m in depth) obviously destroyed any pre-existing structure, but we can suppose that the path heading south on a quite steady and regular downward slope is in fact following the ancient canal. Some small depressions between this path and the head of the first mining structures, highlighted in Figure 18 with blue arrows, can be consistent with this hypothesis.

5. Discussion

5.1. Typo-Morphological Classification of Mining Works

The analysis of these mines makes us identify three main groups of mining structures: horizontal excavations, trenches following the slopes and rock-cut pits and shafts. The latter are related to the exploitation of veins and are only present, in this study area, to the north of Sapeiras mine. They are very common features for the mining of nearly vertical veins. Aerial photographs of 1949 show that the structures visible nowadays are recent. We cannot exclude a former exploration of these veins, at least in their superficial part, even if the mining reports do not mention such vestiges. As they were drafted five years after the 1949 aerial images, any ancient pit would have been erased at that time. In addition, the bedrock here is composed of schists, a friable rock that favours collapses and the consequent disappearance or important modification of mining structures. These are adverse conditions for the preservation and documentation of old vestiges.

Roughly horizontal mining work and excavations following the slopes were both dug on alluviums. The latter are present in the Rasas mine. This type of excavation, on the eastern slope, represents the main part of the mine, with high volumes of sediments removed. The structures are open from an elevation of 60 m to the north and 50 m to the south. They reach the bottom of the valley between 30 and 18 m in elevation. These excavations can be related to the mining of the T2 terraces [39,43] (Figure 8).

The last category of mining structures, characterised by the excavation of the ground down to a certain elevation, can be registered in Sapeiras, Zolas and in some parts of Rasas mine. In those cases, miners extended the work area but did not go below a certain elevation. In Sapeiras mines, they removed the ground mainly between 72 and 65 m. A second horizontal level was reached in the long structure of step 3, to the southeast of the western sector, between 65 and 60 m in elevation. In Zolas and Rasas mines, we can observe a coincidence of these levelled mining structures. In Zolas, it is between 60 and 40 m as a maximum extent and in Rasas, between 60 and 47 m in elevation for the northern large excavated pits and between 48 and 40 m for the platform in the southern sector. We should also include in this range the small area of superficial mining to the north of Rasas mine, between 62 and 61 m in elevation.

The morphology of the mines has a strong relation with the morphology of the mineralised bodies, whether in rock mines or in alluvium terrains [11,51–53]. The fact that in Sapeiras and Zolas mines the miners decided to stop work at a certain elevation may have been related to local changes in the grade of the alluvium in the deeper levels. However, in Rasas mine we observe both the horizontal excavations and the excavations following the slopes. If the grade of ore was also low in the deeper parts, we can suppose that miners had a more efficient way to process the sediments and could obtain sufficient

cassiterite even in deeper excavations. We also need to consider that these two ways of mining implied different ways of managing the digging and the tailings evacuation. This could, therefore, indicate a more complex reorganisation of the mining practices. If these two ways of mining occurred in a short period or having a long period of abandonment of the mines in between, it cannot be ascertained for the moment.

It is also noteworthy that miners of the 20th-century focused their interest on the alluviums close to the watercourses, in the lower parts of the valleys, while in previous, more ancient periods, they worked on the upper terraces. Ancient mines in the lower parts may have also existed, but the more recent mines would have erased them. In addition, the important volume of tailings transported to the lower places when mining in the upper terraces could also have covered previous mines and prevented further work by the accumulation of barren sediments. This might explain why the pits reported in the mining projects close to Sapeiras, Zolas and Rasas mines did not seem to be successful, as no traces of them can be seen in the USAF 1958 aerial images. They were indeed located around ancient tailings. This typo-morphological approach gives indications about the geological knowledge of the miners and about their choices in the organisation of the works. Changes in this organisation may be related to different periods of activity but cannot be related to a specific time period. In fact, this can be compared with Roman and Medieval alluvial mining (e.g., [4,9,14,54–57]). Further investigation, including archaeological excavations, would be necessary to ascertain chronological considerations.

5.2. The Question of Water Supply

The water supply is a key element for the understanding of the organisation of these ancient mines in secondary deposits [58]. The elevation of the mines in relation to the surrounding terrain and watercourses determines the kind of infrastructure necessary to bring the water to the digging sector. In the Rasas mine, the hydraulic network could be quite simple, considering the actual location of watercourses (Figure 18). The situation is different in Sapeiras and Zolas mines. In Sapeiras, the small water tank and its canal are the few clear elements that we can link to hydraulic structures. The small watercourse springing to the north of the mine could have supplied this small tank. According to military maps, it starts at an elevation a little lower than the canal (67 instead of 69 m), but the topographic map of the mining concession shows that this stream flows from a higher elevation (70 m), along the road (Figure 20). We can suppose that the works to build the road affected the upper course of this stream and are responsible for its current low level of flowing. Nevertheless, some problems remain. First, this watercourse has little flow and seems to be dry in summer, as we could observe during ground-truthing works. This might have been different several centuries ago. Secondly, the maximal level of the stream would be 70 m. This remains below the highest elevation of the western sector of this mine, up to 73 m. In the eastern sector, the highest elevation of the mine is 67 m, which would have been within reach of the stream, even without its northern extension. However, the problem here is the depression going down to 62 m between the eastern sector of the mine and the upper part of the ridge to the north. A channel of around 200 m in length and up to 5m in height would have been necessary to save this depression (Figure 20). This would have been a huge structure, standing out even more compared with the relatively reduced volume of these mining works. No architectural remains are visible now on site, nor are they described in the mining archives. The postulated channel, necessary to bring water to this mining sector, is therefore no more than a hypothesis.

As we explained above, Zolas mine is surrounded in all directions by lower terrains. Considering this, the channels needed to bring water from far, from an elevation high enough to reach the top of the mine. The higher part of the mining structures reaches 60 m in elevation. The closest place where some water could be caught at a suitable level, to the south of the eastern sector of Sapeiras mine, is distant more than 500 m and would have to be up to 35 m high (Figure 20). However, the amount of water available from the small stream there does not seem suitable to supply the whole Zolas mine. Another option (we

discarded other ones to the east, even further afield), with a stronger stream, would have been to catch the water from the watercourse flowing in the north. This would have needed a channel of nearly 700 m in length, but only up to 20 m in height (Figure 20). Both options seem, however, quite unlikely: it is expectable that such a channel (from one direction or the other) would have left some remains, which is not the case.

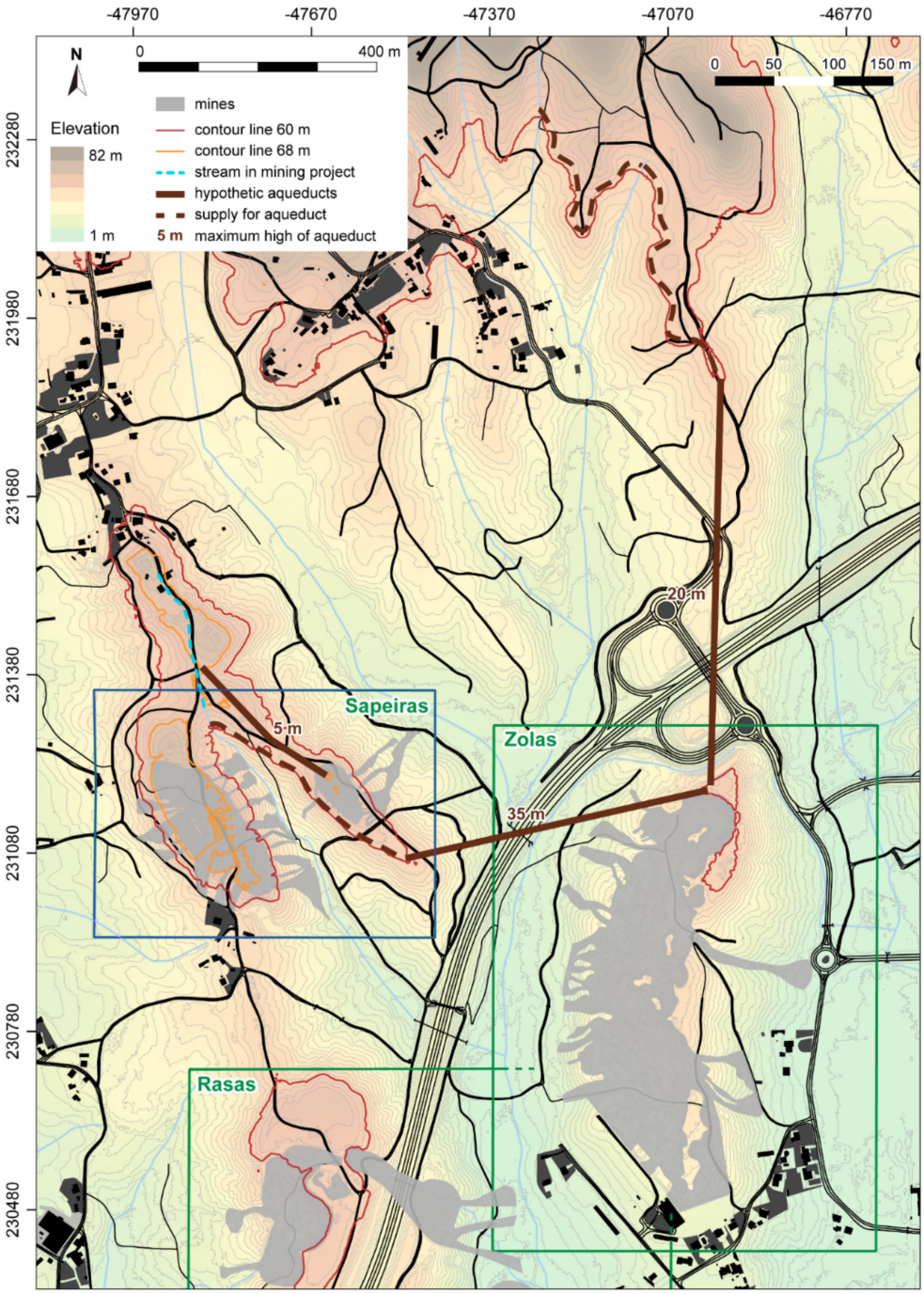

Figure 20. General view of the relief around Sapeiras and Zolas mine, overlapped with 1:10,000 vector cartography of the Viana do Castelo Municipality.

Confronting this issue, we want to highlight the rather weak structure of the alluvium in those mines. The paths and roads provide some cuts across the natural ground close to the ditches or trenches, and we could observe that it is easy to dig in it with simple metallic tools. In addition, we could note that modern mining projects never mention the use of machinery for digging purposes: the miners are supposed to use simple pickaxes

and shovels. Therefore, we suppose that the ground in Zolas and Sapeiras mine could have been at least partly dismantled using manual tools. In that case, water would have been necessary only to wash the sediments to separate the cassiterite from the clay, and to a less extent for digging purposes. In this context, the small water tank of Sapeiras and those we propose in Zolas mine could have their place. The fact that the overall mining structures appear to have been dug by water-powered means would be a consequence of the shape of the excavations combined with the action of steady raining episodes, with a high potential of erosive action. Some landforms resulting from the combination of mining structures and natural processes have also been described recently for the alluvium gold mines in the Teleno mountain [8]. These hypotheses regarding the Viana do Castelo tin mines would, however, need to be confirmed by further geomorphological investigations on these mines.

5.3. Historical Implications

The ground-sluicing technique, well studied in gold mines in northwestern Iberia, is commonly related to the Roman imperial period and to the direct implication of the imperial administration in gold exploitation [4,58,59]. However, in the context of tin mines, we believe that this link between Roman imperial administration and alluvium mines should not be automatic. First, and even considering the Roman influence in the adoption of this technique, we must remember that *Decimus Junius Brutus* crossed the Lima river around 137 BC (App. Iber. 71-73). This early contact could have resulted in an increased demand for local tin and the transmission to and application by indigenous communities of this water-powered technique before the Imperial period. Indeed, the earliest use of hydraulic mining is reported in northern Italy by the *Salassi* and was dated in the 2nd century BC (Strab. Geogr. 4.6.7). The corresponding knowledge was available in the Roman world since that period and could be implemented in the conquered territories [5,60–62].

Another element is that tin, unlike gold, was not under the monopoly of the Roman state [59]. We cannot rule out that local people knowing the resources controlled these mines. The Carvalhelhos hillfort (Boticas, northern Portugal) provides indeed an example of tin production by local people during the 1st century BC associated with early contacts with the Roman world [63]. Finally, similar structures in tin mines have been dated in the Medieval period in other parts of Europe, such as Germany and France [54,55]. Thus, we must consider that those mines could be later than the Roman period, as for their whole activity or only part of it.

6. Conclusions

The integration of remote-sensing techniques such as airborne LiDAR and archival aerial photography with historical maps and documentation, as well as with geological data, has allowed us to review the tin mining landscape of the Tinto valley, an area surrounding the mountain range of Serra d'Arga in northern Portugal. This methodological approach proved to be efficient for mapping the mining traces and for defining a typology of the remains. LiDAR data provided a general visualization of the current state of the structures, allowing us to assess their level of preservation or recent changes. It was also the most useful tool to map the mining remains. Historical maps available for the mining concessions projects are not very accurate and do not show the real extent of the mining works of the 20th century. Nevertheless, they are a useful indication of the sectors where modern mining affected more likely archaeological remains. Aerial imagery, especially from the years 1958 and 1965, corresponding to the time of the mining projects, is an interesting complement to the historical maps. Indeed, the overall absence of deforested areas in those pictures shows that the local concessions did not have a huge impact. The 3D reconstruction from archival aerial imagery also allowed comparisons with LiDAR-derived topography and led to the confirmation that the largest mining structures were not a result of modern activity. In addition, all recent ground alterations could be identified on the different sets of aerial imagery available and considered in the interpretation of data.

However, the vegetation of this northern Portuguese area, with abundant eucalyptus and pine trees on the one hand, and very dense shrubs due to the abandonment of rural land on the other, contributed locally to a decrease in the quality of the LiDAR data. Therefore, it was not always possible to map precisely some of the mining remains. This affected above all the smallest structures, such as canals and small mounds or pits, as in Sapeiras and Zolas mines, and prevented a more precise description of the internal organisation of the mines. The three sets of aerial orthoimages from different decades helped to compensate for this problem, but as soon as 1949, the main part of the mines was already covered by trees. This phenomenon increased in more recent times, with implications for ground-truthing.

Geological sampling and XRF analyses have confirmed the presence of cassiterite on all the three mines. It shows that if these mines were being worked since ancient times, cassiterite would have been the main mineral being exploited.

The three mining sites studied in the Tinto valley present several mining phases, from three to four. However, we have no data about the chronology of each phase nor about the time elapsed between each one. The typology of the mines can be partly consistent with what is known about the Roman imperial period, namely for the ground-sluicing technique, but also for the Medieval one. We also want to highlight the possibility that this activity may have started before the Augustan period, due to the early contacts of the local population with the Roman army.

Regarding the techniques, in Sapeiras and Zolas, the miners worked following horizontal levels, a choice which could be related to changes in the quantity of cassiterite at deeper levels. In Rasas, the main part corresponds to deep excavations on the slopes, implying a different way of managing the mine. The water supply for mining does not represent a problem in the Rasas mine. In Sapeiras and Zolas, the situation is not clear, and we can consider that at least part of the work was done by hand. The water would still have been needed to wash the sediments, in smaller amounts than for digging. This configuration seems to remain out of the Roman alluvium mines typology. Further field study including excavations and absolute dating would be necessary to make chronological precise proposals. The present work, with remote-sensing techniques, would be useful to choose the most suitable locations for these excavations.

Concluding, the present study allowed a relative chronology of the mining areas, by differentiating modern works from older ones. The topographical and morphological details derived from remote-sensing data provided elements to propose a relative chronology of mining phases/steps in the older/ancient mining areas, despite the absence of absolute dating chronologies. In the future, archaeological excavations and absolute dating methods integrated with geological and geomorphological approaches would be necessary to fully comprehend the antiquity, continuity and mining technologies employed in the mines of this region.

Author Contributions: Conceptualization, J.F. and E.M.; methodology, J.F., E.M., J.A.G., F.D., A.L., L.G.-S. and E.F.; investigation, J.F., E.M., J.A.G., F.D., A.L., L.G.-S. and E.F.; writing—original draft preparation, J.F., E.M., J.A.G., F.D., A.L., L.G.-S. and E.F.; writing—review and editing, J.F., E.M., J.A.G., F.D., A.L., L.G.-S. and E.F. All authors have read and agreed to the published version of the manuscript.

Funding: This research was funded by FEDER through the COMPETE 2020 Programme, Lisboa Regional Programme and European Regional Development Fund (FEEI), and National Funds through FCT (Fundação para a Ciência e Tecnologia) under the scope of the Iberian Tin project (PTDC/HAR-ARQ/32290/2017). Part of this work was also funded by National Funds through the FCT under the scope of the project UIDB/50025/2020-2023 to CENIMAT/i3N. J.F. was funded by a Marie Skłodowska-Curie Individual Fellowship (grant agreement No 794048) under the European Union's Horizon 2020 research and innovation programme. F.D. was funded by National Funds through FCT, and co-financed by the European Social Fund (ESF) through POCH – Programa Operacional Capital Humano – and NORTE 2020 Regional Program (ref. 2020.05534.BD).

Data Availability Statement: Restrictions apply to the availability of the presented data.

Acknowledgments: We are grateful to the CIM Alto Minho for providing the airborne LiDAR data of the Viana do Castelo district and to the Viana do Castelo Municipality for providing the 1:10,000 vector cartography. We want to thank the archive service of the Direção-Geral de Energia e Geologia for facilitating our access to the mining reports. A special thanks to Ioana Oltean for her help on the English review of this paper and for her insightful comments.

Conflicts of Interest: The authors declare no conflict of interest.

References

1. Comendador Rey, B.; Meunier, E.; Figueiredo, E.; Lackinger, A.; Fonte, J.; Fernández Fernández, C.; Lima, A.; Mirão, J.; Silva, R.J.C. Northwestern Iberian tin mining from bronze age to modern times: An overview. In *The Tinworking Landscape of Dartmoor in a European Context*; Newman, P., Ed.; Dartmoor Tinworking Research Group: Sowton, UK, 2017; pp. 133–153.
2. Meunier, E. El estaño del Noroeste ibérico desde la Edad del Bronce hasta la época romana. Por una primera síntesis. In *La ruta de las Estrímnides: Navegación y Conocimiento del Litoral Atlántico de Iberia en la Antigüedad*; Ferrer Albelda, E., Ed.; Monografías de Gahia; Universidad de Alcalá: Sevilla, Spain, 2019; pp. 280–320.
3. Domergue, C.; Hérail, G. *Mines d'Or Romaines d'Espagne: Le District de la Valduerna (León)*; Université de Toulouse-Le Mirail: Toulouse, France, 1978.
4. Domergue, C. *Les Mines de la Péninsule Ibérique dans l'Antiquité Romaine*; École Française de Rome: Rome, Italy, 1990; Volume 127.
5. Sánchez-Palencia, F.J.; Vaudagna, A.; Pecharromán, J.L.; Beltrán, A.; Currás, B.; Alonso, F.; Ruiz del Árbol, M. La zona minera de la Bessa (Biella, Italia) como precedente republicano de la minería del oro en *Hispania*. In *Arqueología, Sociedad, Territorio y Paisaje: Estudios Sobre Prehistoria Reciente, Protohistoria y Transición al Mundo Romano en Homenaje a Mª Dolores Fernández Posse*; Bueno, P., Gilman, A., Martín Morales, C., Sánchez-Palencia, F.J., Eds.; Bibliotheca Praehistorica Hispania: Madrid, Spain; CSIC: Madrid, Spain, 2011; pp. 329–347.
6. Currás, B.; Ruiz del Árbol, M.; Sánchez-Palencia, F.J.; Orejas, A.; Romero, D. Ancient landscapes of north-western Iberia: Historical aerial photographs and the interpretation of Iron Age and Roman territories. In *Revovering Lost Landscapes*; Ivanišević, V., Veljanovski, T., Cowley, D., Kiarszys, G., Bugarski, I., Eds.; Institute of Archaeology: Belgrade, Serbia, 2015; pp. 67–68.
7. Cauuet, B.; Boussicault, M. Apport du Lidar à l'étude des mines d'étain antiques en dépôts secondaires autour d'Autun (71). *Bull. Archéologique d'Autun* **2015**, 31–33.
8. Fernández-Lozano, J.; Carrasco, R.M.; Pedraza, J.; Bernardo-Sánchez, A. The anthropic landscape imprint around one of the largest Roman hydraulic gold mines in Europe: Sierra del Teleno (NW Spain). *Geomorphology* **2020**, *357*, 107094. [CrossRef]
9. Fernández-Lozano, J.; Gutiérrez-Alonso, G.; Fernández-Morán, M.A. Using airborne LiDAR sensing technology and aerial orthoimages to unravel roman water supply systems and gold works in NW Spain (Eria valley, León). *J. Archaeol. Sci.* **2015**, *53*, 356–373. [CrossRef]
10. Fernández-Lozano, J.; Gutiérrez-Alonso, G. Improving archaeological prospection using localized UAVs assisted photogrammetry: An example from the Roman Gold District of the Eria River Valley (NW Spain). *J. Archaeol. Sci. Rep.* **2016**, *5*, 509–520. [CrossRef]
11. Fernández-Lozano, J.; Palao-Vicente, J.J.; Blanco-Sánchez, J.A.; Gutiérrez-Alonso, G.; Remondo, J.; Bonachea, J.; Morellón, M.; González-Díez, A. Gold-bearing Plio-Quaternary deposits: Insights from airborne LiDAR technology into the landscape evolution during the early Roman mining works in north-west Spain. *J. Archaeol. Sci. Rep.* **2019**, *24*, 843–855. [CrossRef]
12. Fonte, J.; Pires, H.; Gonçalves-Seco, L.; Matías Rodríguez, R.; Lima, A. Archaeological research of ancient mining landscapes in Galicia (Spain) using Airborne Laser Scanning data. In *Actas do Simpósio Internacional Paisagens Mineiras Antigas na Europa Ocidental: Investigação e Valorização Cultural*; Fontes, L., Martins, C., Eds.; Câmara Municipal de Boticas: Boticas, Portugal, 2014; p. 198.
13. Matías, R.; Llamas, B. Use of LIDAR and photointerpretation to map the water supply at the Las Murias-Los Tallares Roman gold mine (Castrocontrigo, León, Spain). *Archaeol. Prospect.* **2018**, *25*, 59–69. [CrossRef]
14. Matías, R.; Llamas, B. Analysis using LIDAR and photointerpretation of Las Murias-Los Tallares (Castrocontrigo, León-Spain): One of the biggest Roman gold mines to use the "Peines" system. *Geoheritage* **2019**, *11*, 381–397. [CrossRef]
15. Matías, R.; Llamas, B. Roman gold mining at "Las Miédolas" (NW Spain): Lidar and photo interpretation in the analysis of "Peines" system. *Geoheritage* **2021**, *13*, 29. [CrossRef]
16. Almeida, C.A.B. *Proto-Historia e Romanização da Bacia Inferior do Lima*; Faculdade de Letras do Porto: Porto, Portugal, 1990.
17. Moreira, M.A.F. As "Arrugiae" da época romana no vale do rio Tinto do concelho de Viana do Castelo. In *I Colóquio Galaico-Minhoto*; Galaico-Minhota, A.C., Ed.; Câmara Municipal de Ponte de Lima: Ponte de Lima, Portugal, 1981; Volume II, pp. 395–423.
18. Moreira, M.A.F. A Romanização do litoral do Alto Minho. *Caminiana* **1982**, *VI*, 31–96.
19. Alves, R. Contribuição para um Sistema de Gestão Integrada de Sítios Mineiros do NW de Portugal. Ph.D. Thesis, Universidade do Minho, Braga, Portugal, 2014.
20. Servicios Politécnicos Aéreos (SPASA). *Voo LiDAR: Proposta Metodológica*; Servicios Politécnicos Aéreos: Madrid, Spain, 2018.
21. Servicios Politécnicos Aéreos (SPASA). *Relatório de Voo Combinado LiDAR e Foto*; Servicios Politécnicos Aéreos: Madrid, Spain, 2018.
22. Lozić, E.; Štular, B. Documentation of archaeology-specific workflow for airborne LiDAR data processing. *Geosciences* **2021**, *11*, 26. [CrossRef]
23. Hesse, R. LiDAR-derived local relief models—A new tool for archaeological prospection. *Archaeol. Prospect.* **2010**, *17*, 67–72. [CrossRef]

24. Kokalj, Ž.; Somrak, M. Why not a single image? Combining visualizations to facilitate fieldwork and on-screen mapping. *Remote Sens.* **2019**, *11*, 747. [CrossRef]
25. Zakšek, K.; Oštir, K.; Kokalj, Ž. Sky-view factor as a relief visualization technique. *Remote Sens.* **2011**, *3*, 398–415. [CrossRef]
26. Boehner, J.; Koethe, R.; Conrad, O.; Gross, J.; Ringeler, A.; Selige, T. Soil regionalisation by means of terrain analysis and process parameterisation. In *Soil Classification 2001*; Micheli, E., Nachtergaele, F., Montanarella, L., Eds.; Research Report; European Soil Bureau: Luxembourg, 2002; pp. 213–222.
27. Boehner, J.; Selige, T. Spatial prediction of soil attributes using terrain analysis and climate regionalisation. In *SAGA—Analysis and Modelling Applications*; Boehner, J., Mc Cloy, K.R., Strobl, J., Eds.; Goettinger Geographische Abhandlungen: Goettingen, Germany, 2006; pp. 13–28.
28. BergWerkGIS. VoGIS-Profil-Tool. Available online: https://github.com/BergWerkGIS/VoGIS-Profil-Tool/ (accessed on 20 August 2021).
29. Redweik, P.; Roque, D.; Marques, A.; Matildes, R.; Marques, F. Triangulating the past—Recovering Portugal's aerial images repository. *Photogramm. Eng. Remote Sens.* **2010**, *9*, 1007–1018. [CrossRef]
30. Karara, H.M.; Abdel-Aziz, Y.I. Accuracy aspects of non-metric imageries. *Photogramm. Eng. Remote Sens.* **1974**, *40*, 1107–1117.
31. Pinto, A.T.; Gonçalves, J.A.; Beja, P.; Pradinho Honrado, J. From archived historical aerial imagery to informative orthophotos: A framework for retrieving the past in long-term socioecological research. *Remote Sens.* **2019**, *11*, 1388. [CrossRef]
32. Gonçalves, J.A. Automatic orientation and mosaicking of archived aerial photography using structure from motion. *Int. Arch. Photogramm. Remote Sens. Spat. Inf. Sci.* **2016**, *XL-3/W4*, 123–126. [CrossRef]
33. Blanco-Rotea, R.; Costa-García, J.M.; Fonte, J.; Gago Mariño, M.; Gonçalves, J.A. A Modern Age redoubt in a possible Roman camp. The relationship between two defensive models in Campos (Vila Nova de Cerveira, Minho Valley, Portugal). *J. Archaeol. Sci. Rep.* **2016**, *10*, 293–308. [CrossRef]
34. Fonte, J.; Costa-García, J.M. Alto da Cerca (Valpaços, Portugal): Um assentamento militar romano na Serra da Padrela e sua relação com o distrito mineiro de Tresminas. *Estudos do Quaternário* **2016**, *15*, 39–58. [CrossRef]
35. Fonte, J.; Lima, A.; Matías Rodríguez, R.; Gonçalves, J.A.; Leal, S. Novas evidências de mineração aurífera e estanhífera de época romana no alto vale do Tâmega (Montalegre e Boticas, norte de Portugal). *Estudos do Quaternário* **2017**, *17*, 45–55. [CrossRef]
36. Fonte, J.; Pimenta, J.; Pereira, C.; Arruda, A.M. Revisitando os Chões de Alpompé com técnicas de deteção remota: Novas evidências sobre os sistemas defensivos Romano-Republicanos. *Cuadernos de Prehistoria y Arqueología* **2020**, *46*, 215–238. [CrossRef]
37. Potere, D. Horizontal positional accuracy of Google Earth's high-resolution imagery archive. *Sensors* **2008**, *8*, 7973–7981. [CrossRef]
38. Amorim, A.B.C.; Freitas, J.A.G. O arquivo das minas do Norte de Portugal (1839–2011). Construção do arquivo digital de informações. *Boletim de Minas* **2015**, *50*, 75–92.
39. Caetano Alves, M.I. Terraços fluviais do Alto Minho: Bacia do rio Lima e depósitos de Alvarães. *Memória do Museu e Laboratório Mineralógico e Geológico* **1995**, *4*, 395–399.
40. Caetano Alves, M.I.; Insua Pereira, D. A sedimentação e a gliptogénese no registo cenozóico continental do Minho (NW Portugal). *Ciências da Terra UNL* **2000**, *14*, 99–110.
41. Leal Gomes, C. Estudo Estrutural e Paragenético de um Sistema Pegmatóide Granítico—O Campo Filoniano de Arga—Minho (Portugal). Ph.D. Thesis, Universidade do Minho, Braga, Portugal, 1994.
42. Rodríguez Fernández, L.R.; López Olmedo, F.; Oliveira, J.T.; Medialdea, T.; Terrinha, P.; Matas, J.; Martín-Serrano, A.; Martín Parra, L.M.; Rubio, F.; Marín, C.; et al. Mapa Geológico de la Península Ibérica, Baleares y Canarias a Escala 1/1.000.000. 2015. ©Instituto Geológico y Minero de España (IGME); ©Laboratório Nacional de Energia e Geologia (LNEG). Available online: https://info.igme.es/cartografiadigital/geologica/ (accessed on 29 January 2021).
43. Caetano Alves, M.I. Análise dimensional de sedimentos fluviais: Formação de Alvarães e depósitos de terraços da bacia do rio Lima (NW de Portugal). *Estudos do Quaternário* **1999**, *2*, 65–72. [CrossRef]
44. Caetano Alves, M.I. Alves, M.I. A sedimentação Fluvial Cenozóica na região do Minho (Portugal). In *Encontros Sobre a Geomorfologia do Noroeste Peninsular*; Faculdade de Letras da Universidade do Porto, Gedes: Porto, Portugal, 2002; pp. 19–21.
45. Teixeira, C.; Medeiros, A.C.; Coelho, A.P. *Noticia Explicativa da Folha 5-A Viana do Castelo*; Serviços Geológicos de Portugal: Lisboa, Portugal, 1972.
46. Machado, J.V.; (Mining engineer of Circunscrição mineira do Norte, Porto, Portugal). *Dossier n.º 2946. Mina de Estanho, Denominada Cobalto N.º 2, Concessionada à Mineira Estrela de Rocha, Lda, Freguesia Vila Mou, Concelho Viana do Castelo*, Unpublished report. 1954.
47. Machado, J.V.; (Mining engineer of Circunscrição mineira do Norte, Porto, Portugal). *Dossier n.º 3238. Mina de Estanho, Denominada Cruz de Lenta, Concessionada à Mineira Estrela de Rocha, Lda, Freguesia Meixedo, Concelho Viana do Castelo*, Unpublished report. 1958.
48. Machado, J.V.; (Mining engineer of Circunscrição mineira do Norte, Porto, Portugal). *Dossier n.º 3239. Mina de Estanho, Denominada Balteiro N.º1, Concessionada à Mineira Estrela de Rocha, Lda, Freguesia Meixedo, Concelho Viana do Castelo*, Unpublished report. 1958.
49. Anonymous; (Chief mining engineer of Circunscrição mineira do Norte, Porto, Portugal). *Alto da Bouça da Breia*, Unpublished report. 1955.
50. Sánchez-Palencia, F.J. La zona minera de Penamacor-Meimoa (Castelo Branco). In *Minería Romana en Zonas Interfronterizas de Castilla y León y Portugal*; Sánchez-Palencia, F.J., Ed.; Junta de Castilla y León: León, Spain, 2014; pp. 103–133.
51. Domergue, C. *Les Mines Antiques*; Picard: Paris, France, 2008.

52. Cauuet, B.; Tamas, C.-G. Les travaux miniers antiques de Rosia Montana (Roumanie). Apports croisés entre archéologie et géologie. In *Minería y Metalurgia Antiguas: Visiones y Revisiones. Homenaje a Claude Domergue*; Orejas, A., Rico, C., Eds.; Collection de la Casa de Velázquez; Casa de Velázquez: Madrid, Spain, 2012.
53. Fabre, J.-M.; Meunier, E.; Souhassou, M.; Rico, C.; Antolinos Marín, J.A. La mina romana de plomo argentífero de la Rambla del Abenque (Sierra Minera de Cartagena): Morfología de los trabajos de extracción, tipos de mineralización y cronología de la explotación. In *Presente y Futuro de los Paisajes Mineros del Pasado: Estudios Sobre Minería, Metalurgia y Poblamiento*; García Pulido, L., Arboledas Martínez, L., Alarcón García, E., Contreras Cortés, F., Eds.; Editorial Universidad de Granada: Granada, Spain, 2017; pp. 131–139.
54. Tolksdorf, J.F.; Schröder, F.; Petr, L.; Herbig, C.; Kaiser, K.; Kočár, P.; Fülling, A.; Heinrich, S.; Hönig, H.; Hemker, C. Evidence for Bronze Age and Medieval tin placer mining in the Erzgebirge mountains, Saxony (Germany). *Geoarchaeol. Int. J.* **2019**, *35*, 198–216. [CrossRef]
55. Dessolin, T.; Cauuet, B. Les anciennes mines d'étain de l'Autunois: Actualité des recherches. *Bull. Archéologique d'Autun* **2018**, *2018*, 47–59.
56. Cauuet, B.; Tamas, C.-G.; Boussicault, M. Le district stannifère d'Autun. *Les Dossiers d'Archéologie* **2006**, *316*, 26–27.
57. García Pulido, L.J. La minería hidráulica romana desarrollada en el Cerro del Sol (Granada) para explotar sus recursos auríferos. *Cuadernos de la Alhambra* **2008**, *43*, 76–101.
58. Sánchez-Palencia Ramos, F.J.; Orejas Saco del Valle, A.; Sastre Prats, I.; Pérez, L.C. Las zonas mineras romanas del Noroeste peninsular. Infraestructura y organización del territorio. In *Nuevos Elementos de Ingeniería Romana, Proceedings of the III Congreso de las Obras Públicas Romanas, Astorga, Spain, 5–7 October 2006*; Moreno Galli, I., Ed.; Junta de Castilla y León: León, Spain; Consejería de Cultura y Turismo: Madrid, Spain, 2006; pp. 265–285.
59. Hirt, A.M. *Imperial Mines and Quarries in the Roman World: Organizational Aspects 27 BC–AD 235*; Oxford University Press: Oxford, UK, 2010.
60. Gianotti, F. Geological setting of the Pleistocene placers and roman gold mines of the Ivrea Morainic Amphitheatre (Piedmont, NW Italy). *Ital. J. Quat. Sci.* **2011**, *24*, 183–185.
61. Sánchez-Palencia, F.J.; Vaudagna, A.; Pecharromán, J.L.; Iriarte, E. *La Minería Romana de Oro en Italia: La Bessa (Biella) Como Precedente Republicano de la Minería en Hispania. Informes y Trabajos. Excavaciones en el Exterior 2012*; Ministerio de Educación, Cultura y Deportes: Madrid, Spain, 2014; Volume 11, pp. 55–72.
62. Bannon, C. Fresh water in Roman law: Rights and policy. *J. Rom. Stud.* **2017**, *107*, 60–89. [CrossRef]
63. Figueiredo, E.; Fonte, J.; Lima, A.; Veiga, J.P.; Silva, R.J.C.; Mirão, J. Ancient tin production: Slags from the Iron Age Carvalhelhos hillfort (NW Iberian Peninsula). *J. Archaeol. Sci.* **2018**, *93*, 1–16. [CrossRef]